2014-01-01

Combustion SynThesis Of Molybdenum Silicides And Borosilicides For Ultrahigh-Temperature Structural Applications

Mohammad Shafiul Alam
University of Texas at El Paso, msalam@miners.utep.edu

COMBUSTION SYNTHESIS OF MOLYBDENUM SILICIDES AND BOROSILICIDES FOR ULTRAHIGH-TEMPERATURE STRUCTURAL APPLICATIONS

MOHAMMAD SHAFIUL ALAM

Department of Mechanical Engineering

APPROVED:

Evgeny Shafirovich, Ph.D., Chair

Yirong Lin, Ph.D.

David A. Roberson, Ph.D.

Charles H. Ambler, Ph.D.
Dean of the Graduate School

COMBUSTION SYNTHESIS OF MOLYBDENUM SILICIDES AND BOROSILICIDES FOR ULTRAHIGH-TEMPERATURE STRUCTURAL APPLICATIONS

by

Mohammad Shafiul Alam, B.Sc.

THESIS

Presented to the Faculty of the Graduate School of

The University of Texas at El Paso

in Partial Fulfillment

of the Requirements

for the Degree of

MASTER OF SCIENCE

Department of Mechanical Engineering

THE UNIVERSITY OF TEXAS AT EL PASO

August 2014

Acknowledgements

I would like to extend my gratitude to several people who have been instrumental in helping me complete this thesis. First and foremost to Dr. Evgeny Shafirovich, whose faithful advice and guidance have brought me to this point; it was an honor to work under him.

This research is supported by the U.S. Department of Energy (Grant DE-FE-0008470) and Climax Molybdenum, Inc. as cost sharing partner. I would like to express my gratitude to them.

I want to thank the committee members, Dr. Yirong Lin and Dr. David Roberson who has been a faithful advisor throughout my research.

I specially thank my teammates Alan Esparza, Armando Delgado, Ashvin Kumar Narayan Swamy, Daniel Rodriguez, and Marco Machado for their continuous support and assistance throughout my research.

Finally, I would like to thank *c*SETR and Department of Mechanical Engineering for all their support.

Abstract

Molybdenum silicides and borosilicides are promising structural materials for gas-turbine power plants. A major challenge, however, is to simultaneously achieve high oxidation resistance and acceptable mechanical properties at high temperatures. For example, molybdenum disilicide ($MoSi_2$) has excellent oxidation resistance and poor mechanical properties, while Mo-rich silicides such as Mo_5Si_3 (called T_1) have much better mechanical properties but poor oxidation resistance. One approach is based on the fabrication of $MoSi_2$–T_1 composites that combine high oxidation resistance of $MoSi_2$ and good mechanical properties of T_1. Another approach involves the addition of boron to Mo-rich silicides for improving their oxidation resistance through the formation of a borosilicate surface layer. In particular, Mo_5SiB_2 (called T_2) phase is considered as an attractive material. In the thesis, $MoSi_2$–T_1 composites and materials based on T_2 phase are obtained by mechanically activated SHS. Use of SHS compaction (quasi-isostatic pressing) significantly improves oxidation resistance of the obtained $MoSi_2$–T_1 composites. Combustion of Mo–Si–B mixtures for the formation of T_2 phase becomes possible if the composition is designed for the addition of more exothermic reactions leading to the formation of molybdenum boride. These mixtures exhibit spin combustion, the characteristics of which are in good agreement with the spin combustion theory. Oxidation resistance of the obtained Mo–Si–B materials is independent on the concentration of Mo phase in the products so that the materials with a higher Mo content are preferable because of better mechanical properties. Also, T_2 phase has been obtained by the chemical oven combustion synthesis technique.

Table of Contents

List of Tables

List of Figures

Chapter 1: Introduction

1.1 MOLYBDENUM SILICIDES AND BOROSILICIDES AS MATERIALS FOR UNLTRAHIGH-TEMPERATURE STRUCTURAL APPLICATIONS

The ever present aspiration to enhance the efficiency of gas-turbine power plants by operating at higher temperatures leads to the demand for new, ultrahigh-temperature structural materials. In current turbines, components made of nickel-based superalloys can reach temperatures approaching 1150 °C, which is about 200 °C below their melting points. Gas temperatures within the turbines can be higher when the parts are protected by cooling systems and thermal barrier coatings, but cooling drastically reduces the actual engine performance. A preferred solution is the development of new structural materials, based on molybdenum silicides and borosilicides, which can operate at temperatures higher than 1300 °C as well as provide better performance.

1.1.1 Need for New Ultrahigh-temperature Structural Materials

For many years, investigations have been going on to introduce new materials for high temperature structural applications. Currently, nickel-based superalloys are widely used in gas turbine power plants as these alloys allow improved performance and better efficiency. However, the limited operating temperatures due to lower melting point (1350°C) lead to the search of alternatives to these alloys. Nickel-based alloys possess many attractive properties like high tensile strength, sufficient ductility, and good oxidation resistance. So, in order to replace these superalloys, the new alternatives should match or surpass the performance. In that perspective, metals with high melting point such as Mo alloyed with Si have been treated as promising alternatives [1].

1.1.2 Advantages and Disadvantages of $MoSi_2$

$MoSi_2$ has been recognized as a promising high-temperature structural material. It

possesses a combination of many properties that make it attractive as a high-temperature material. $MoSi_2$ possesses properties similar to ceramic such as excellent oxidation resistance at higher temperature. Also, it possesses metal-like electrical conductivity. Due to combination of attractive properties such as a high melting point (2030°C), reasonable density (6.24 g/cm^3), excellent high temperature oxidation resistance, and a brittle-to-ductile transition in the vicinity of 900°C, $MoSi_2$ can be used in oxidizing environments at temperatures that significantly exceed 1100°C, the limit for current nickel-based superalloys. Further, $MoSi_2$ is non-toxic, environmentally benign, and, due to a relatively high electrical conductivity, suitable for electro-discharge machining (EDM) [2].

Currently, $MoSi_2$ is widely used as heating elements in electric furnaces, in production environment for the production of glass, steel, electronics, ceramics, and in heat treatment of materials because it can withstand up to 1800 °C. It is also used in microelectronics as contact materials. Besides these applications, $MoSi_2$ has been recognized as a promising high-temperature structural material for advanced boilers and turbines where the temperature requirement is very high and environment is highly oxidizing.

A single $MoSi_2$ phase, however, cannot be used in structural applications because of poor mechanical properties. Like ceramics, it shows brittleness at room temperature leading to poor fracture toughness. Also, at elevated temperatures, it provides poor creep resistance. Low fracture toughness at room temperature and low strength at elevated temperatures, however, hinder widespread use of $MoSi_2$ in structural applications [2-7]. So, in order to use $MoSi_2$ for high-temperature structural applications, it is necessary to improve these properties.

1.1.3. Methods for Improvement of $MoSi_2$ Properties

Promising solutions for improving the mechanical properties of $MoSi_2$ are based on the incorporation and control of secondary phases [8, 9]. $MoSi_2$ can be alloyed with other high melting point silicides such as Mo_5Si_3, WSi_2, $NbSi_2$, $CoSi_2$, and Ti_5Si_3 [2]. It is also thermodynamically stable with a wide variety of potential ceramic reinforcements for

composites, including SiC, Si_3N_4, Al_2O_3, ZrO_2, TiB_2, and TiC [2].

A number of encouraging results have been obtained for some materials. The addition of 50 mol% WSi_2 to $MoSi_2$ increased the yield stress at 1500°C by a factor of 8-10 [10] and also remarkably improved the hardness and toughness of $MoSi_2$ matrix at room temperature [11]. Silicon carbide (SiC) is excellent oxidation-resistant reinforcement and yields encouraging mechanical property improvements. For example, by the incorporation of SiC, the room temperature fracture toughness was improved from 2.5 to 9 $MPa.m^{1/2}$ [12]. The creep properties of $MoSi_2$ have also been successfully enhanced by the addition of SiC whiskers and particles [6].

Other intermetallics in the Mo-Si system have been investigated as an alternative to $MoSi_2$; in particular, Mo_5Si_3, also called T_1 phase according to the phase diagram (see figure 1.1) has been studied extensively.

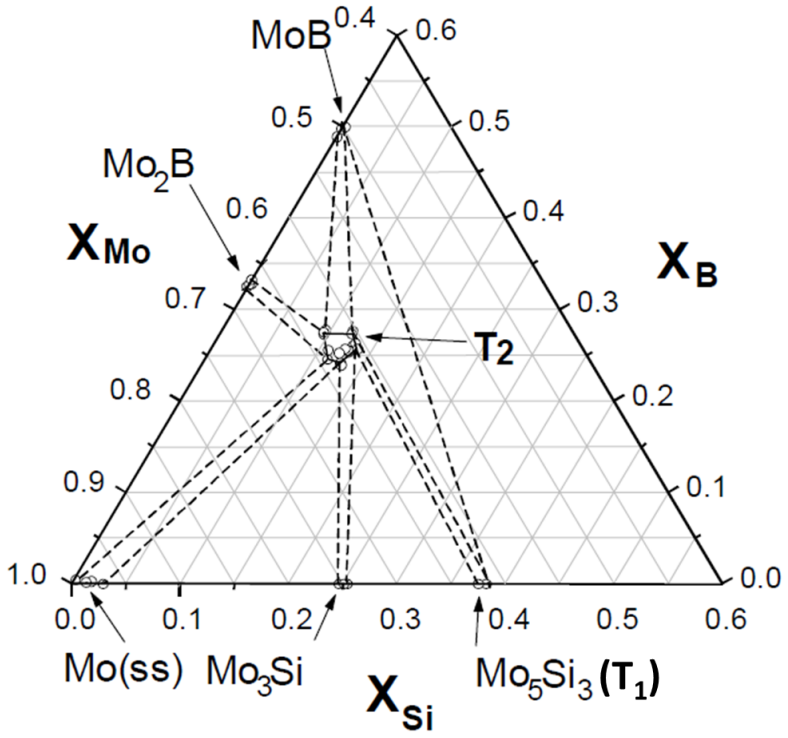

Figure 1.1: Isothermal section (1600°C) of the molybdenum-rich portion of the Mo-Si-B phase diagram [13].

The composite of $MoSi_2$ – 50 mol% Mo_5Si_3 shows a seven-fold increase in the yield strength at 1200°C over the monolithic $MoSi_2$ [4]. However, although mechanical properties of Mo-richer silicides such as Mo_5Si_3 and Mo_3Si are better, they have lower oxidation resistance [14]. This is associated with the formation of volatile oxide MoO_3 in Mo-rich materials.

One approach to the improvement of oxidation resistance of Mo-rich silicides is the addition of boron [15]. Working on the foundation laid by Nowotny et al.[13] who developed the Mo-Si-B ternary phase diagram (see Figure 1.1), Berczik [15] discovered that silicon and boron added in small amounts drastically improve the oxidation resistance of molybdenum while still retaining its favorable high-temperature strength. This is attributed to the formation of a borosilicate glass surface layer, which is highly protective to transport of oxygen. Currently, Mo_5SiB_2 (called T_2) phase is considered as a promising component of advanced materials for ultrahigh-temperature structural applications [1, 13-17]. For example, one promising material is a three-phase mixture of Mo solid solution (α-Mo_{ss}), $A15$ (Mo_3Si) and T_2 (Mo_5SiB_2) where Mo_{ss} phase enhances toughness and the intermetallic phases provide oxidation resistance. All three phases have the melting point above 2000°C, are thermodynamically stable, and exhibit significant resistance to coarsening at elevated temperatures.

1.1.4 Fabrication of $MoSi_2$-based Materials

This study is focused on the fabrication of $MoSi_2$-Mo_5Si_3 composites and materials based on Mo_5SiB_2 phase. A unique feature of this study is the use of combustion synthesis techniques such as mechanically activated self-propagating high-temperature synthesis (MASHS) and SHS compaction. The goal of using these techniques is to develop a novel and competitive processing route for manufacturing ultrahigh-temperature structural materials based on molybdenum silicides and borosilicides.

1.2 SELF-PROPAGATING HIGH-TEMPERATURE SYNTHESIS (SHS)

Self-propagating high-temperature synthesis, commonly known as SHS, is a technique that has been used to primarily to fabricate a wide range of alloys and metal composites. This

process involves the propagation of a high-temperature zone through a compact of reactants. In SHS, the highly exothermic reaction between the reactants is the driving force. SHS has been receiving significant attention by many research groups. However, to achieve a high degree of microstructural control in SHS is very challenging since it involves intense reaction rates. To be considered as a potential fabrication technique, there are some challenges that should be addressed regarding process economics, residual porosity, and reproducible microstructures and properties.

1.2.1 Classic SHS

Self-propagating high-temperature synthesis is an attractive technique to fabricate $MoSi_2$–T_1 composites and T_2 phase. This process is sustained by the heat of the exothermic reaction between constituent powders.

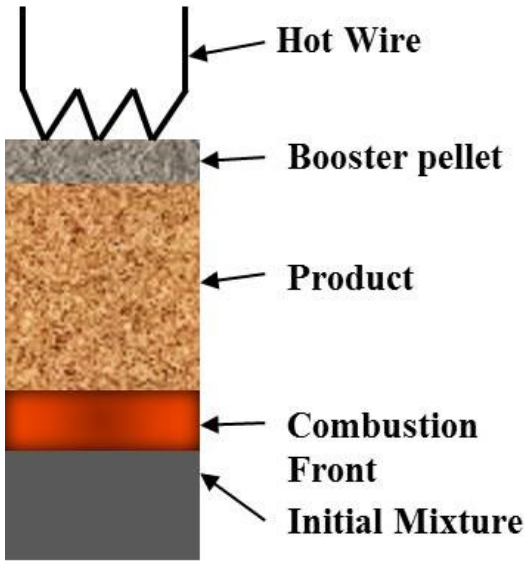

Figure 1.2: Self-propagating high-temperature synthesis.

During SHS process, energy input is required to start ignition only. Upon ignition, the exothermic reaction generates sufficient heat that causes self-propagation of the combustion front throughout the remaining mixture (Fig 1.2). So the major advantage of conventional SHS is

low energy consumption. As the energy problems become more alarming, the harnessing of heat released by the process may be viewed as a step in right direction [18]. Other advantages of SHS include simple and inexpensive equipment, short processing time, tailored microstructures and properties, and higher purity of the products [18-20].

1.2.2 Mechanically Activated SHS

A major problem of using conventional SHS for the fabrication of $MoSi_2$-based materials is low exothermicities of the initial mixtures. The adiabatic combustion temperature of the mixture 1 mol Mo and 2 mol Si is 1913 K (calculated at 1 atm using THERMO software [21]). This allows a self-sustained combustion, but the required increase in Mo concentration decreases the exothermicity to the level where conventional SHS is impossible unless the mixture is preheated [22-25]. Preheating needs either electricity or an additional, highly exothermic system around the mixture (a "chemical oven"). Both options diminish SHS advantages such as low energy and low cost. The low exothermicity problems can be overcome or at least reduced with the so-called mechanically activated SHS (MASHS), which was successfully used for synthesis of $MoSi_2$ [26, 27] and other compounds [18].

The method adds a short-duration high-energy ball milling step, which precedes the combustion process. The high-energy milling, also called mechanical activation, rapidly produces nanostructured powders, so that intermixing of reactive components is obtained on a nanometric scale. The fracture-welding process during milling increases the contact surface area between reactants and destroys the oxide layer on their surface. As a result, mechanical activation improves the reaction kinetics, leading to an easier ignition and stable combustion. The MASHS technique combines the advantages of mechanical alloying (which is typically a multi-hour procedure) and SHS. It also allows for the formation of materials that cannot be obtained by either of these techniques if used alone.

1.2.3 SHS Compaction

SHS compaction involves densification of the SHS products to obtain dense, non-porous, and stronger materials. SHS compaction involves different methods for densification. One of the most promising techniques is quasi-isostatic pressing. This SHS densification process involves uniaxial pressing of SHS products. This technique is based on the standard hydraulic or mechanical pressing equipment. In this process pressure is applied through a pressure-transmitting medium (PTM) to the products by means of a press. The most commonly used PTM are sand and mixture of alumina and graphite powder.

1.3 RESEARCH OBJECTIVES

The goal of this study is to develop a novel and competitive processing route for manufacturing materials based on $MoSi_2$ and Mo_5SiB_2 that are promising candidates for using as structural materials in advanced fossil energy applications. Specifically, this study investigates the use of mechanically activated self-propagating high-temperature synthesis followed by compaction for fabricating these materials. The objectives of this research are:

- To explore the feasibility of fabricating $MoSi_2$–Mo_5Si_3 and Mo_5SiB_2–based composites by mechanically activated SHS.
- To explore the feasibility of fabricating dense composites using SHS compaction.
- To explore the feasibility of fabricating stoichiometric Mo_5SiB_2 in chemical oven combustion synthesis technique.
- Determine mechanical and oxidation properties of the materials produced by MASHS-compaction.

Chapter 2: Literature Review on Different Techniques for Fabrication and Densification of $MoSi_2$-based Composites

2.1 FABRICATION METHODS

To fabricate $MoSi_2$ and $MoSi_2$-based composites, various methods have been used such as arc-melting and casting, hot pressing, reactive sintering, mechanical alloying, spray processing, solid-state displacement reactions, chemical vapor deposition, exothermic dispersion, shock synthesis, and self-propagating high-temperature synthesis (SHS), also called combustion synthesis [6, 12]. Further improvements in the microstructure and behavior of $MoSi_2$ are possible through the judicious combination of several synthesis techniques [12]. In this context, a recently developed technique, called ***mechanically activated self-propagating high-temperature synthesis (MASHS)***, is of great interest [26, 27].

2.1.1 Mechanical Alloying

Mechanical alloying has been used extensively, in recent years, for the synthesis and fabrication of $MoSi_2$. Mechanical alloying is a process that involves repeated fracturing and welding of elemental powders during high-energy milling (Fig. 2.1) [28].

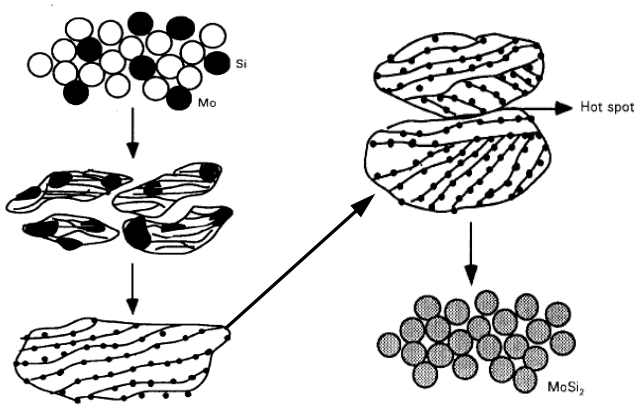

Figure 2.1: Schematic of $MoSi_2$ compound formation by mechanical alloying [28].

Four basic stages constitute this process: (i) stage 1: extreme cold welding; (ii) stage 2: rapid fracturing, creating lamellae; (iii) stage 3: second stage cold welding, resulting more convoluted lamellae; (iv) final stage: a steady state period.

Iwatomo and Uesaka first reported the formation of $MoSi_2$ by mechanical alloying of Mo and Si powders [29]. In this study, it was reported that mechanical alloying provided highly refined crystalline $MoSi_2$ with a grain size of 5 to 10 nm. Although, compared to the other techniques, these products did not exhibit any significant improvement in mechanical and electrical properties, it should be noted that the final density exceeded 97% of the theoretical density.

Jayashankar and Kaufman [30] reported the synthesis of in-situ SiC-reinforced $MoSi_2$ composites using mechanical alloying. In their work, Mo and Si powders were mixed with 4 wt% of C for mechanical alloying. The microstructures of the alloyed powders were highly homogenous and clean.

Schwarz et al. [31] studied mechanical alloying for the synthesis of $MoSi_2$-based alloys. Following their study, they reported some advantages of mechanical alloying technique such as higher density, lower hot-pressing temperatures for consolidation, better microstructure, and improved mechanical properties at room temperature.

However, synthesis of silicides in mechanical alloying usually forms amorphous SiO_2 phase, which is critical in applications requiring very good creep properties. Also, mechanical alloying is limited to very small quantities so that large-scale production becomes difficult. Another problem is contamination of the powders by gases and environments. Moreover, mechanical alloying is a time-consuming process.

2.1.2 Shock Synthesis

In shock synthesis process, a high-energy shock wave is applied to facilitate reactions in a mixture of elemental powders. Shock synthesis of mixtures undergoes extensive plastic deformation and particle comminution, leading to homogenous and clear microstructures.

Yu and Mayers used shock synthesis and successfully synthesized molybdenum disilicides (Fig. 2.2) [32]. However, the products exhibited a large porosity.

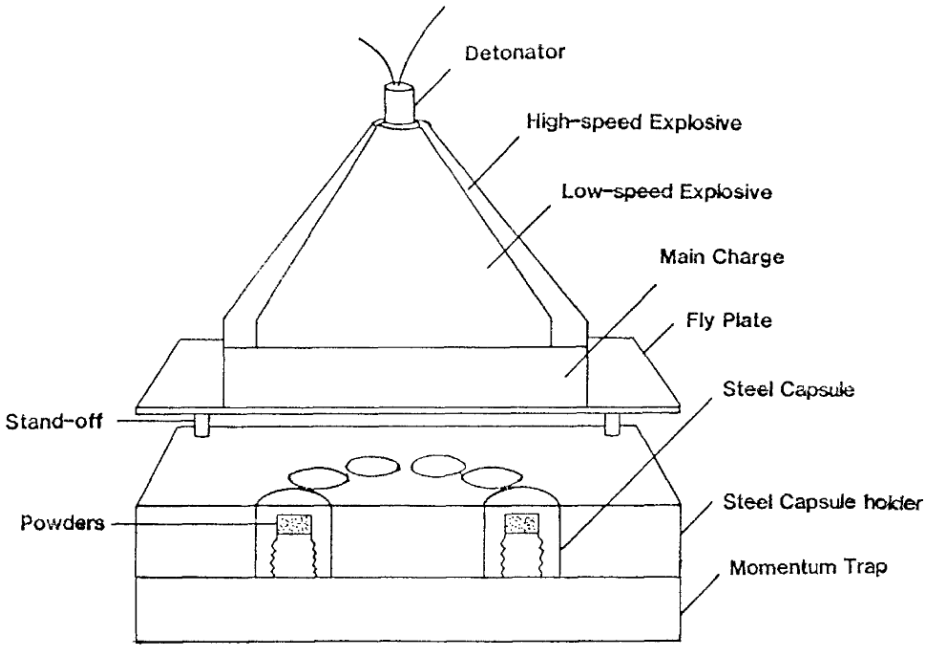

Figure 2.2: The cross-section of the shock processing system used by Yu and Mayers [32].

2.1.3 Chemical Vapor Deposition

Chemical vapor deposition involves the formation of a coating from vapor phase reactants. This process is commonly used to deposit coatings on a heated substrate for improving mechanical and electrical properties. Pierson et al. reported the use of chemical vapor deposition technique to deposit molybdenum silicides [??].

2.1.4 Combustion synthesis

Various intermetallic compounds can be synthesized by combustion synthesis technique. This technique uses the heat of exothermic reaction between the constituent powders. During this process, the reaction is initiated at the top or bottom of the sample. Then the self-propagating

reaction occurs and combustion front propagates throughout the sample without additional energy.

Combustion synthesis has been used by many research groups to fabricate molybdenum silicides and borosilicides. Deevi in 1991 studied self-propagating high-temperature synthesis to fabricate single phase $MoSi_2$ from elemental Mo and Si powders [33]. In their experiments, the maximum combustion temperature was equal to 1886 K, very close to the adiabatic flame temperature (1900 K). The product was confirmed as a single-phase $MoSi_2$ and the purity of the product was very high as compared to the reactants with significantly reduced oxygen impurity. This study has not provided any mechanical and microstructural analysis.

Zhang and Munir (1991) investigated SHS for the synthesis of molybdenum silicides such as Mo_3Si, Mo_5Si_3, and $MoSi_2$ [23]. $MoSi_2$ reacted in a self-sustaining mode without any prior heating. However, the other silicides reacted only with preheating. The activation energy for $MoSi_2$ was 139.4 KJ/mol which was significantly lower than the other silicides.

Another investigation of SHS was carried out to produce Mo_5Si_3 in a chemical furnace (Fig. 2.3) [24]. 5Ti + 3Si mixture was used as the chemical fuel. The study confirmed the formation of single-phase Mo_5Si_3.

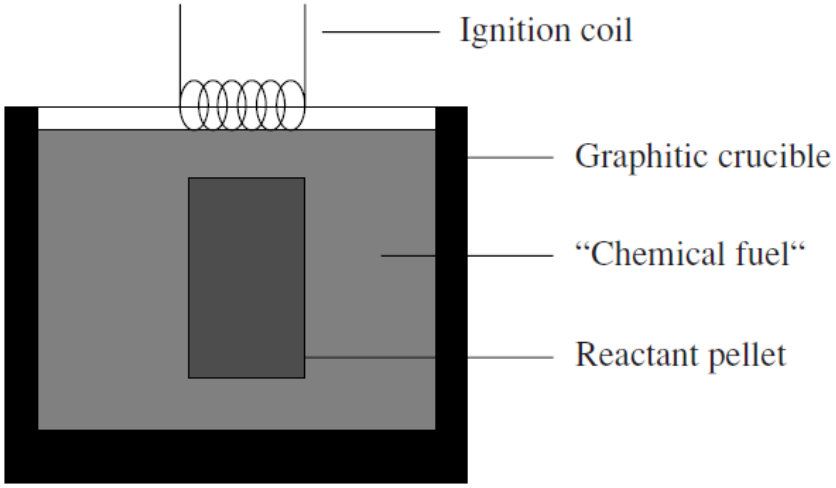

Figure 2.3: Schematic diagram of the chemical furnace used for combustion synthesis [24].

A recent study by Yeh and Chen involved the preparation of $MoSi_2$ and $MoSi_2$–Mo_5Si_3 composites by SHS [25]. Six different compositions corresponding to the Si content in the range of 45.5–66.7 at% were tested. Experimental results concluded that the starting stoichiometry and preheating temperature greatly affects the propagation mode of the combustion front, the combustion wave velocity, and the reaction temperature. Chrysanthou et al. also successfully investigated combustion synthesis of $MoSi_2$, $MoSi_2$/TiC and (Mo, W) Si_2 composites [34]

Zhang et al. used both mechanical alloying and self-propagating high-temperature synthesis for fabrication of $MoSi_2$ matrix composites reinforced by WSi_2 and La_2O_3. They concluded that it was difficult to synthesize Mo–W–Si–La_2O_3 powder mixture by mechanical alloying. SHS was found to be more suitable for that composite [11].

2.1.5 Mechanically activated combustion synthesis

Self-propagating high-temperature synthesis becomes more effective when it is combined with mechanical activation of the reactants. A brief literature search on mechanical activation revealed that $MoSi_2$ powders prepared by mechanical activation can be composed of nanostructured particles that do not require a large evolution of chemical composition [27]. Under the same experimental conditions, the combustion front velocity can be increased significantly by mechanical activation compared to that observed in conventional SHS. High-energy ball-milling (mechanical activation) provides pure α-$MoSi_2$ with nanometric structure (D_{MoSi2}= 88 nm).

Gras et al. used MASHS technique to study the combustion wave structure during the production of $MoSi_2$ [26]. In the MASHS process, the reaction $Mo+2Si \rightarrow MoSi_2$ was greatly enhanced by the oxide-free interfaces between Mo and Si. Mechanical activation resulted in special nanostructure that facilitated self-sustained combustion. In addition, mechanical activation enhanced the solid–solid interactions and facilitated the initial SHS reaction by producing sufficient heat. Mechanical activation also ensured a stable combustion wave.

Xu et al. in 2009 worked with mechanical activation followed by combustion synthesis to synthesize $MoSi_2$-SiC composite [35]. Mo and Si nanocrystallites were obtained during the ball-milling process that was easily ignited compared to the unmilled Mo +Si + C mixture and confirmed the formation of $MoSi_2$/SiC composite. Also, a significantly higher combustion temperature was obtained. Different mechanical tests revealed that the composite exhibited good properties with relative density, flexural strength, Vicker's hardness and fracture toughness as 99%, 468.7 MPa, 15.5 GPa and 9.35MPam$^{1/2}$, respectively.

Another study with mechanical activation was performed by Xu et al. in 2010 to synthesize $MoSi_2$/WSi_2 composites [36]. The experimental results confirmed that, like in their previous study with $MoSi_2$/SiC composites, mechanical activation facilitates combustion and $MoSi_2$/WSi_2 composite was successfully synthesized. However, mechanical properties were not studied.

2.1.6 Chemical oven combustion synthesis

Chemical oven combustion synthesis or chemical oven SHS (COSHS) has been used by various researchers for powders that are difficult to ignite in conventional SHS. In COSHS, the main pellet is surrounded by a highly-exothermic booster mixture, which ignites easily. Combustion of the booster mixture generates sufficient amount of heat to ignite the main pellet and ensure its stable combustion.

COSHS was studied to investigate $MoSi_2$ composite reinforced with SiC whiskers powders, produced from the mixing of Mo, Si, carbon black, and Si_3N_4 whiskers [37]. They used mixture of Ti and Si (atomic ratio Si/Ti = 3/5) as the chemical oven. Also, carbon felt was used between the chemical oven and main pellet. Figure 2.4 represents the schematic of the experimental apparatus used in this study.

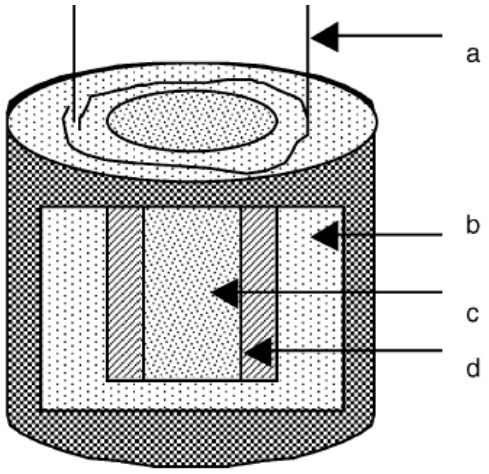

Figure 2.4: Schematic of experimental apparatus used for chemical oven combustion synthesis (a) W coil; (b) 3Si + 5Ti (atomic ratio); (c) 2Si + Mo (atomic ratio); (d) carbon felt [38].

In another study, Xu et al. reported the characterization of $SiC_w/MoSi_2$ composite obtained from COSHSed powder [38]. They Vickers hardness, flexural strength, and fracture toughness of the $SiC_w/MoSi_2$ composite were 11.15 GPa, 457 MPa, and 6.20 $MPa \cdot m^{1/2}$, respectively, which were higher by 26.1%, 134.3% and 47.3%, respectively, than for $MoSi_2$ matrix,. Levashov et al. also used the chemical oven technique for SHS of Mo-B-Si system [39]. Since it is difficult to ignite stoichiometric Mo_5SiB_2, they followed COSHS to ensure complete combustion.

2.2 SHS DENSIFICATION METHODS

Densification of SHS products has been a matter of great concern. Also, SHS of Mo−Si and Mo−Si−B structural materials leads to a high porosity of the combustion products. Usually, SHS products have to be crushed and then re-compacted using conventional methods of powder metallurgy. Porosity depends largely on combustion temperature that can be controlled by internal methods, while SHS products can be pressed externally after combustion. High pressure can be applied to the product immediately after SHS, at high temperatures, to obtain non-porous materials and items of intricate shape. There are several methods to accomplish SHS compaction such as pressureless densification (sintering), dynamic shockwave, and quasi-isostatic pressing [40-43].

2.2.1 Pressureless Densification (Sintering)

During SHS, formation of a liquid phase is observed in some systems. This happens mainly because of the high temperatures generated during SHS. The maximum temperature during combustion can exceed the lower melting point of the intermetallic compound. According to many researchers, by increasing the temperature of the reacting mixture, it is possible to increase density of the combustion product. Here melting of intermetallic compounds produces liquid-phase sintering. In this case, there is no need for applying external pressure. An investigation of such a process has been conducted for Ni + Ti system [44]. At different combustion temperatures, two different combustion modes were observed and the density of the combustion product was influenced by these modes.

The second process for pressureless densification includes milling of SHS products foolowed by sintering of the milled products. Thus, the size of the reactants can be controlled leading to the fabrication of submicron ceramic powders. For Al_2O_3-TiC and Al_2O_3-WC systems, pressureless sintering of the obtained products provided mechanical and microstructural characteristics similar to those of commercially available powders [20]. Although this process includes an additional step, it is cost-effective for fabricating dense materials.

2.2.2 Dynamic Shockwave

Another method of SHS densification is dynamic shockwave or explosive compaction. This method uses explosives to improve product properties. There are two main approaches to perform explosive compaction. Figure 2.5 (a) shows the apparatus that consists of a thin-walled cylinder surrounded by explosives. During detonation, it causes the compaction of the SHS products. In second approach shown in Fig. 2.5 (b), the explosive shockwave causes the movement of a massive piston that leads to the compaction of reaction products. In dynamic shockwave, it is possible to achieve 97 – 99 % of the theoretical density of the material [45].

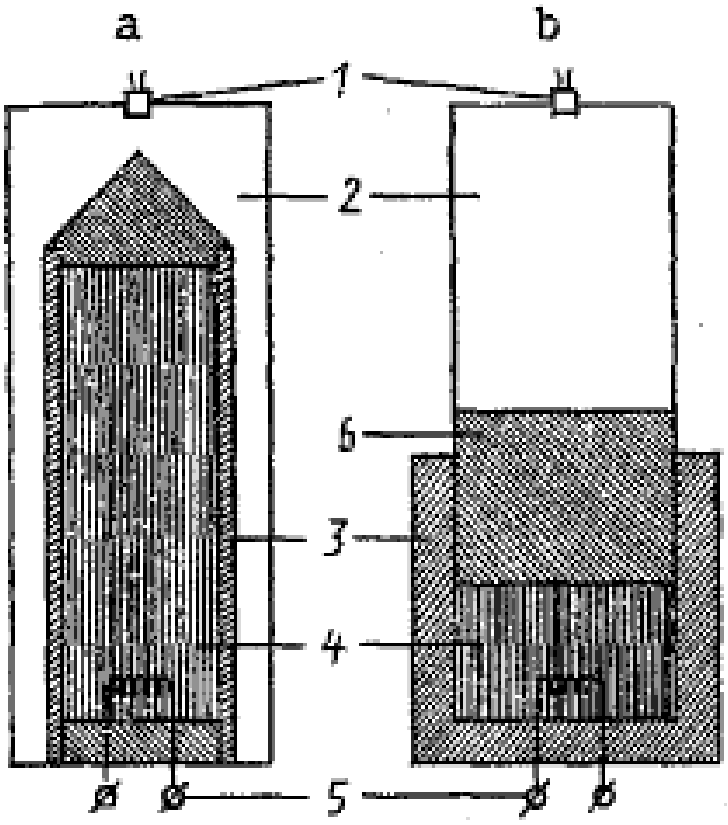

Figure 2.5: SHS dynamic shockwave compaction schemes: 1) electric fuse; 2) explosive; 3) metal container; 4) green mixture; 5) electric ignited; 6) massive piston.

2.2.3 Quasi-Isostatic Pressing

Uniaxial pressing with a pressure-transmitting medium (PTM) (Fig. 2.6) is commonly known as quasi-isostatic pressing (QIP). This process is also known as Ceracon Process. In the patented Ceracon process, both the pressure-transmitting medium (PTM) and the initial mixture are preheated to achieve an isostatic state and higher combustion temperatures. This method has been used in manufacturing sector.

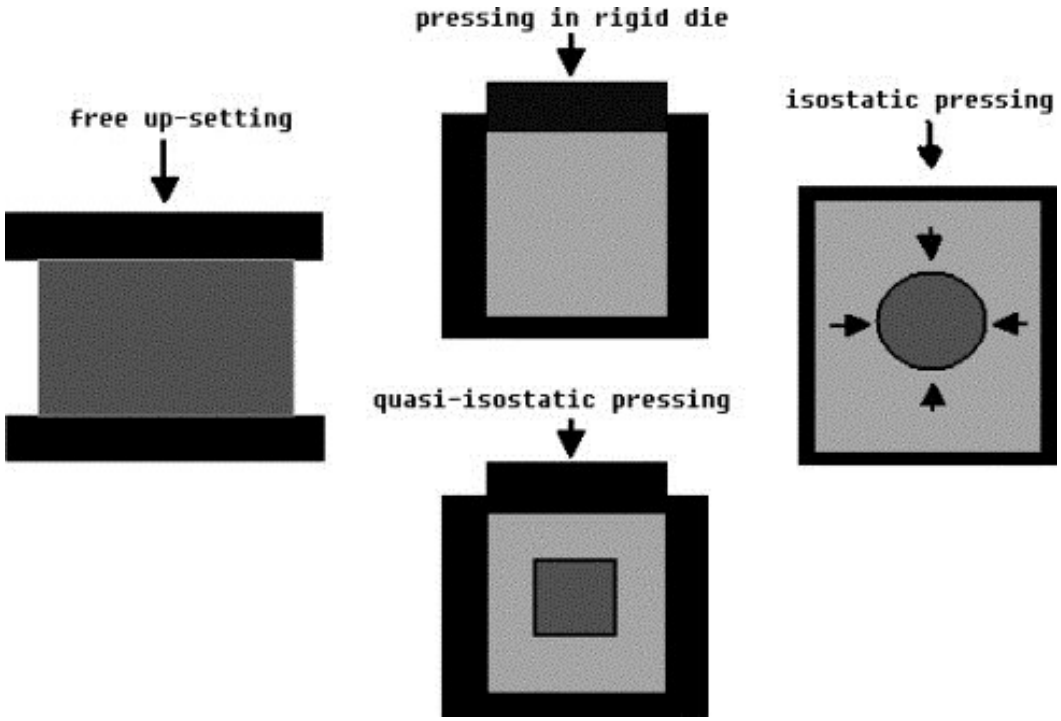

Figure 2.6: Schematics of different densification processes [46].

Recently, the combination of self-propagating high-temperature synthesis (SHS) and quasi-isostatic pressing has attracted attention as a method for producing dense materials. Merzhanov and co-workers are the pioneers of this method [??]. By the combined SHS−QIP method, it is possible to produce hundreds of industrially useful materials with low porosity and high density. In this technique, alumina, silica, or alumina with graphite powder are usually used as the pressure transmitting media (PTM). In addition to be used as the pressure transmitters, these powders also reduce heat loss during SHS by acting as a thermal insulator.

The SHS−QIP method had been used by Xinghong et al. [47] to produce dense TiC/TiB_2 ceramics, an attractive material for aircraft propulsion systems, cutting tools, machine tools, etc. The conventional densification processes that were used previously to produce such ceramics were complicated and expensive. Figure 2.7 represents the SHS densification apparatus used by Xinghong et al. [47]. In their study, pellets made from the mixtures of titanium, B_4C, and carbon powders were placed inside the apparatus. Sand was used as the pressure transmitting medium. A heating coil was connected at one end of the pellet for ignition. After complete combustion of the

pellet, about 160 kPa pressure was applied to the SHS product. It was reported that quasi-isostatic pressing increased the product density to 90-97%. Also, very good mechanical properties were achieved.

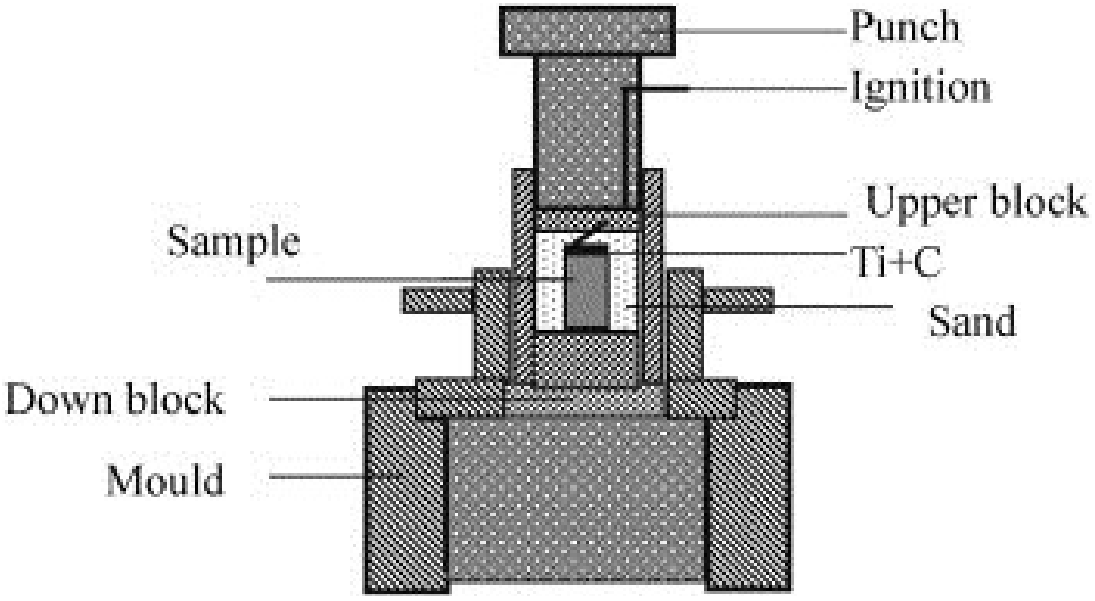

Figure 2.7: Experimental setup of SHS and quasi-isostatic pressing used by Xinghong et al. [47]

Martinez Pacheco reported the use of a combination of SHS and quasi-isostatic pressing for fabricating TiC-NiFe, a promising functional graded material [48]. In this study, Ti, C, and NiFe were mixed according to the composition of 5 to 20 wt% of NiFe with the balance TiC. The mixtures were then compacted into cylindrical pellets. The green pellet was placed inside a die and the remaining space was filled with pressure transmitting medium. Loosely packed mixture of high purity alumina and graphite powders was used as PTM. Figure 2.8 shows the apparatus for SHS compaction used in this study.

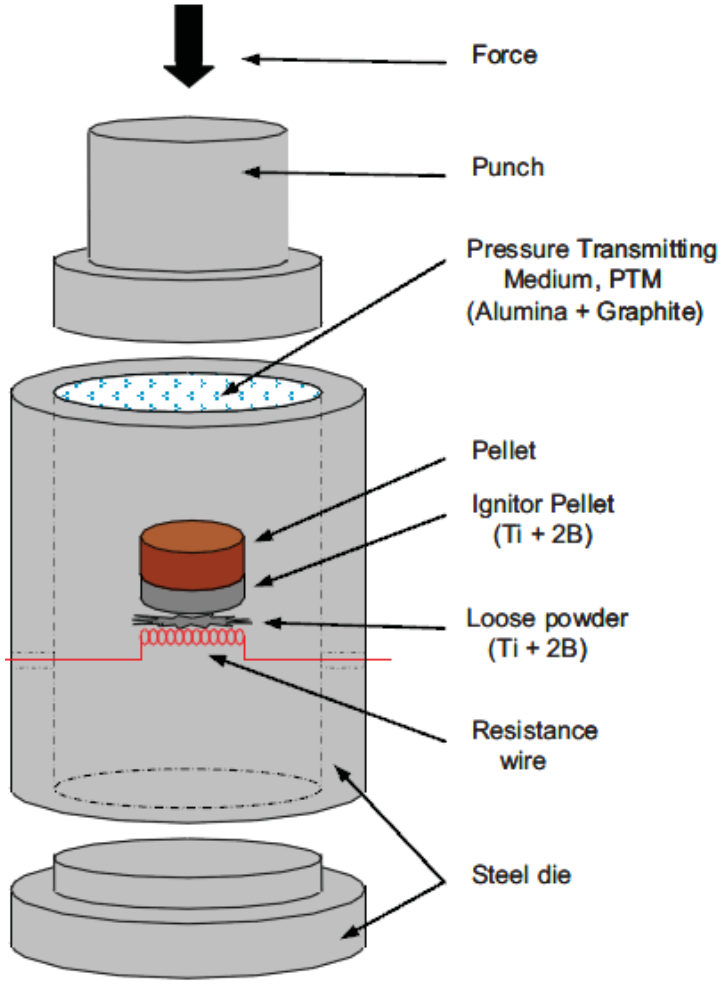

Figure 2.8: Uniaxial pressing SHS compaction schematic used by Martinez Pacheco [48].

A booster pellet made from the stoichiometric mixture of Ti and B (Ti + 2B) was used to start ignition. Initially, this booster pellet was ignited by a resistance wire which was connected to the power supply. After 3 to 6 seconds of ignition of the igniter pellet, SHS process over the green pellet was completed. A jet of PTM escaping from the die provided the indication of ignition. The delay time for compaction, i. e., the time needed for combustion to propagate throughout the pellet was determined in another experiment with the same composition. Two K-type thermocouples were used at the top and bottom of the pellet and average combustion wave velocity was measured. The pressure exerted on the pellet varied from 150 to 400 MPa. The pressing time was 100 seconds.

The product after quasi-isostatic pressing indicated that porosity was predominant in areas with highest ceramic content. Also, the relative density of the product was less than 70% (measured by Archimedes technique). The pressure distribution in the PTM was investigated by small sensor films (10 mm by 5 mm strips) that indicated that instead of being isostatic, it exerted more in the horizontal plane. Further investigation was carried on to improve the densification process as the areas with highest ceramic contents were too porous.

Kvanin et al. used the SHS-QIP technique for the fabrication of dense intermetallic compounds, namely, ɣ-TiAl [49]. In their study, a mixture of 50 at% Ti and 50 at% Al was used as the charge material. After the self-propagating combustion, the sample was compacted with a quasi-liquid medium inside a die with 100 to 200 MPa pressure. The relative density of the final product reached 99%.

Delgado and Shafirovich used the SHS-QIP technique in their study of combustion of JSC-1A lunar regolith with Mg for the production of construction materials on the Moon [42]. They performed quasi-isostatic pressing immediately after combustion that increased the density of the product. The compression test of the final product has shown that the compressive strength was about 10 MPa, higher than that of common brick (5 MPa).

The combination of SHS and pseudo-hot-isostatic pressing (PHIP) was used by Kholghy et al. in their research of producing dense $Al_2O_3/TiB_2/TiC$ multi-ceramic composite [50]. This process resulted in 92.7% relative density of the composite. Also, the hardness and fracture toughness of the product were much stronger than for conventional ceramics.

Another research using QIP was performed by Zhang et al. [51]. They investigated densification of boron carbide ceramics and could densify the samples to 98% of the theoretical density.

2.4 SUMMARY

The development of new high-temperature structural materials for gas-turbine power plants suggests, considering both mechanical and oxidation properties, a need for fabricating molybdenum silicides and borosilisides. It would be attractive to use mechanically activated combustion synthesis for this because it incorporates low energy consumption as well as simple and inexpensive equipment. Also, the chemical oven combustion synthesis technique looks promising for the synthesis of Mo_5SiB_2.

Among the densification methods, quasi-isostatic pressing technique looks promising because of the following:

- Pressureless densification eliminates the need for mechanical work, but it cannot produce fully dense materials.
- Although dynamic shockwave yields greater relative densities, it requires special consideration during experiments since the use of explosives in the lab would require much more safety/hazard analysis and special handling.
- Quasi-isostatic pressing is the most feasible technique as it can be performed in the lab with simplicity, but it requires further optimization to obtain high density materials.

Chapter 3: Experimental Facilities and Techniques

3.1 Sample Preparation

Molybdenum (99.95% pure, Climax Molybdenum), silicon (crystalline, 99.5% pure, Alfa Aesar), and boron (amorphous, 94–96% pure, Alfa Aesar) powders were used in this study. Particle size distributions for these powders were determined with a multi-laser particle size analyzer (Microtrac Bluewave). These measurements have shown that the used molybdenum has the volume mean diameter of 16.64 μm and median diameter of 11.25 μm, while silicon has the volume mean diameter of 10.15 μm and median diameter of 7.72 μm.

3.1.1 Preparation of $MoSi_2$-Mo_5Si_3 Composites

To obtain $MoSi_2$-Mo_5Si_3 composite, a mixture of Mo (34.70 – 44.57 at%) and Si (65.30 – 55.43 at%) was prepared. These mixtures correspond to the expected product composition of 60 − 90 vol% $MoSi_2$ and 10 − 40 vol% Mo_5Si_3 (80.95 - 98.11 mol% $MoSi_2$ and 1.89 – 19.05 mol% Mo_5Si_3).

3.1.2 Preparation of Materials Based on Mo_5SiB_2 Phase

To obtain materials based on Mo_5SiB_2 Phase, a mixture of Mo (58.3 – 62.5 at %), Si (8.3 – 12.5 at %), and B (25 – 33.4 at %) was prepared. These mixtures correspond to the expected product composition of 10 − 67 mol% MoB with the balance Mo_5SiB_2.

The powders were mixed uniformly in a three-dimensional inversion kinematics tumbler mixer (Inversina 2L, from Bioengineering, Inc.) (Fig. 3.1), with the mixing time of 1 h. Usually, 100 g of powders were mixed in one process.

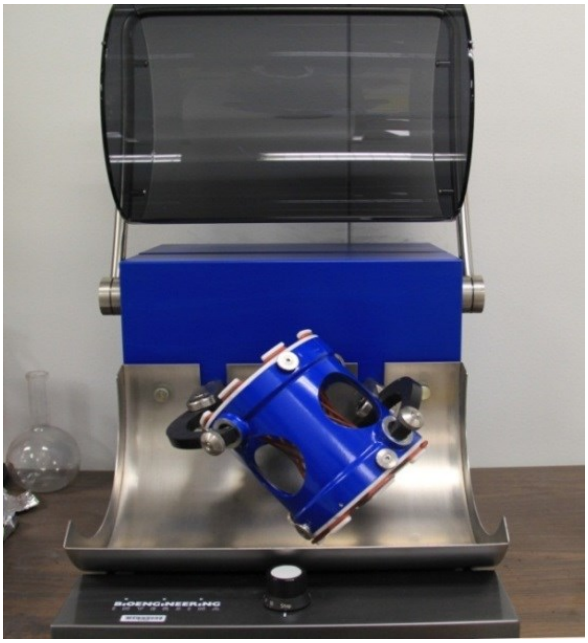

Figure 3.1: Three-dimensional inversion kinematics tumbler mixer (Inversina 2L).

The mixture was then milled in a planetary ball mill (Fritsch Pulverisette 7 premium line) (Fig. 3.2).

Figure 3.2: Planetary ball mill (Fritsch Pulverisette 7 Premium Line).

Zirconia-coated 80-mL bowls were used. The grinding media were 1.5-mm zirconia balls. The milling was conducted in an argon environment using bowls with special lids (Fritsch). The procedure included several milling and cooling cycles, which was necessary to avoid overheating the bowls and the mixture. The mixture to ball mass ratio was equal to 1:6. The milling process included 4 milling-cooling cycles (10 min milling at the maximum rotation speed of 1100 rpm and 75 min cooling).

The as-milled powders were compacted into cylindrical pellets in a uniaxial hydraulic press (Carver) using a 13 or 25-mm-diameter pellet die (Fig.3.3). Usually, the pressing varied from 30–40 kN. The pellet diameter was 13 mm in most experiments. Some SHS compaction tests were also conducted with 25-mm diameter pellets. The pellet height was 20–25 mm. The relative density of the pressed samples was 55–60 %. A booster pellet was also prepared from the stoichiometric titanium/boron (1 mol Ti + 2 mol B) mixture following the same process as the main pellet except that milling was not performed to prepare the booster pellet.

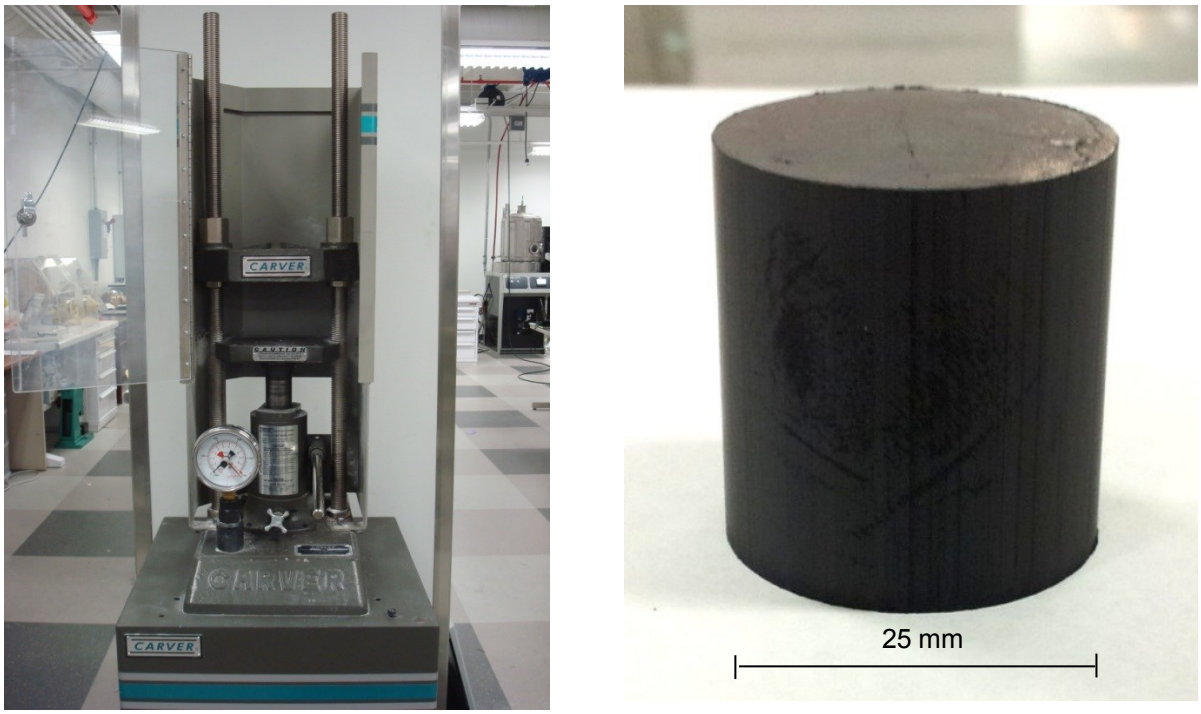

Figure 3.3: Hydraulic press and compressed pellet.

3.2 Experimental Setup and Procedure for SHS in an Argon Environment

For combustion in argon (SHS), the pellet was installed on a ceramic fiber insulator (Fiberfrax) in a 30-L stainless steel reaction chamber (Fig 3.4). A booster pellet was placed at the top of the sample. The chamber was evacuated and filled with ultrahigh purity argon at 1 atm. In that process, the chamber was purged three times using a vacuum pump (Fisher Scientific, Maxima C Plus) and argon. As the pressure in the lab is usually 885 mbar, the pressure inside the chamber was set close to the 2-psi mark in the pressure gauge (138 mbar) to adjust the difference of that to standard ambient pressure.

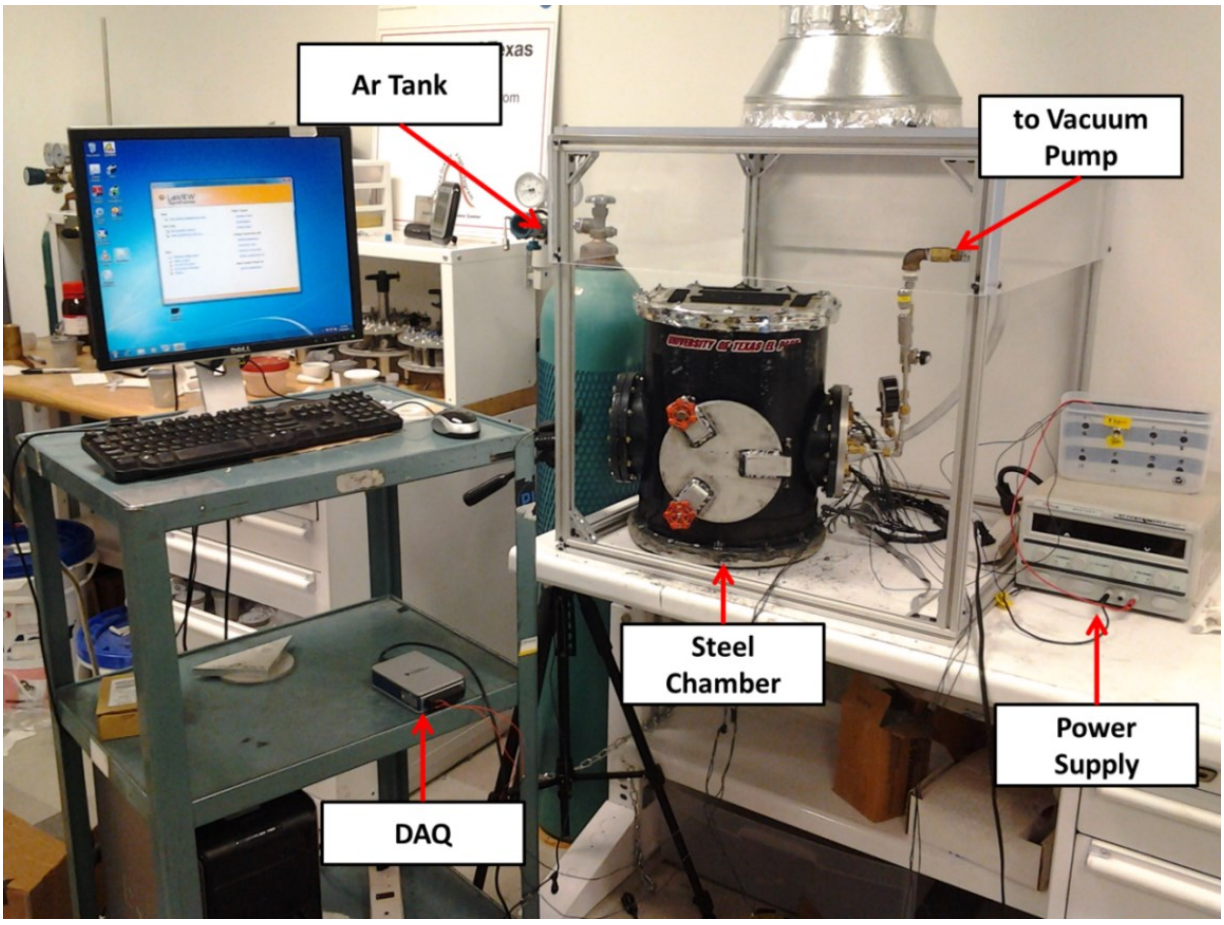

Figure 3.4: Experimental setup for SHS.

The booster pellet was heated by a 0.43 mm-diameter tungsten wire coil (Midwest Tungsten Service Inc.), connected to a DC power supply (Mastech). After fast combustion of the booster mixture, the power supply was shut off. However, propagation of the combustion front over Mo/Si mixture was observed. That means, it didn't need additional energy for the combustion front to propagate throughout the sample. The reaction between the constituent powders sustained the complete combustion. This is an important advantage of SHS that ensures low energy consumption.

Chromel−Alumel thermocouples (type K, wire diameter: 0.25 mm, Omega Engineering) were used to measure the temperature in the middle of the sample during the combustion process. The thermocouples, located in two-channel ceramic insulators, were inserted into pellets through drilled channels. The thermocouples were connected to a USB-based data acquisition system (National Instruments USB-9211). Video recording through a glass window was used for observation of the combustion process and further investigation of combustion behavior.

3.3 SHS COMPACTION

A recently developed cylindrical steel die for SHS compaction [42] was used. The die has an inner diameter of 7 cm and the wall thickness of 2.5 cm (CAD design of the die is shown in Fig. 3.5). There are six horizontal channels in the wall of the cylinder that has the diameter of 2.7 mm. These channels were used for the ignition wires, thermocouples, and removal of gases that may form during combustion. During experiments, upper horizontal channels were kept open for removal of gases, the mid horizontal channels served for thermocouple wires and the bottom channels were used for ignition wires.

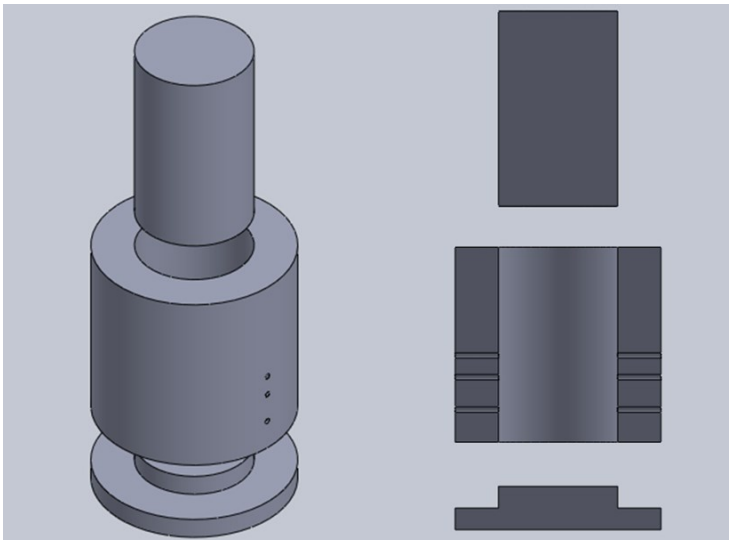

Figure 3.5: CAD design of SHS compaction die.

The pellet was installed inside this die and the igniter (a tungsten wire, folded in a waffle pattern and connected to the power supply) was located at the bottom of the pellet. Silica powder was used as a pressure-transmitting medium. This powder (150 g) was poured into the die to fully surround the pellet (Fig. 3.6)

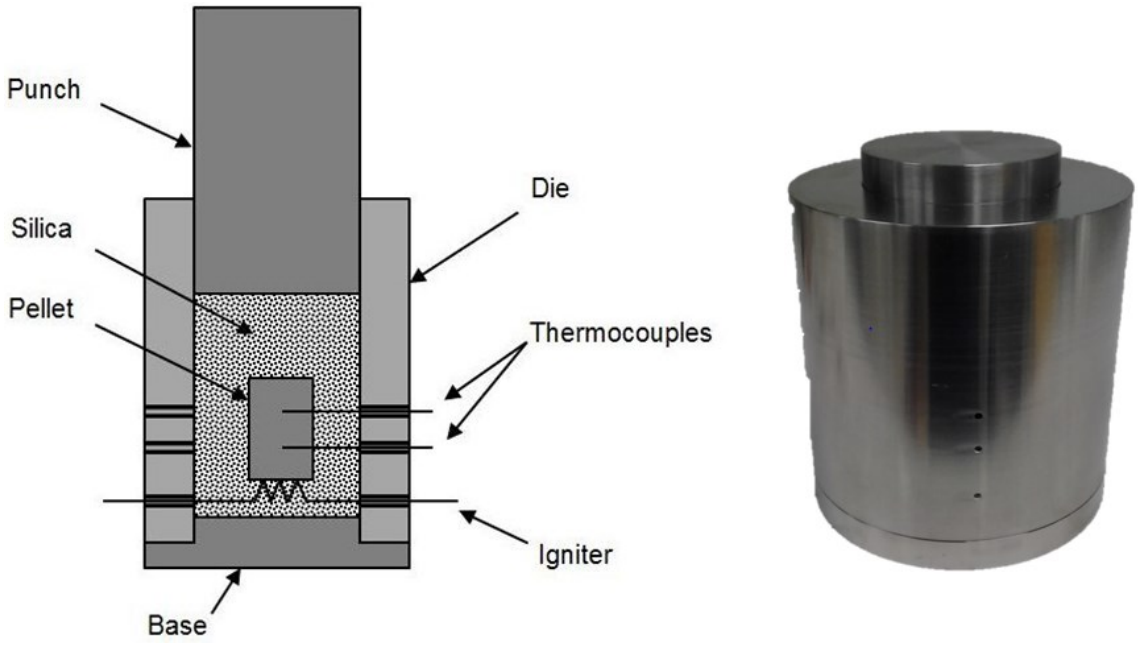

Figure 3.6: SHS compaction apparatus.

The die was placed under the aforementioned hydraulic press (Fig. 3.7). Once ignition was achieved, the power supply was turned off. A jet of silica escaping from the apparatus through one of the horizontal channels indicated that combustion was occurring. Immediately after the end of combustion, the press was operated (force: 60−80 kN). After natural cooling of the die for about one hour, the obtained product pellet was removed. A thin layer of silica, adhered to the pellet surface, was removed using grinding paper.

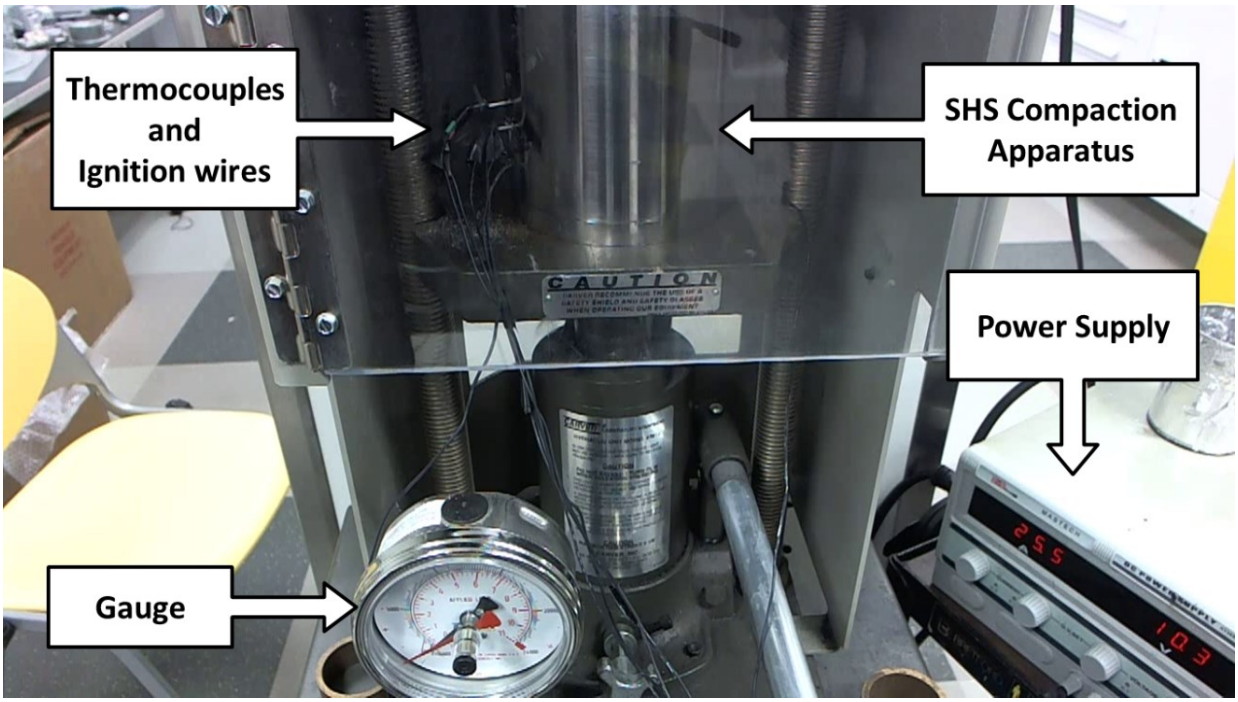

Figure 3.7: Experimental setup for SHS compaction.

3.4 Analysis of Products

3.4.1 X-ray Diffraction Analysis

X-ray diffraction analysis was performed using Bruker D8 Discover XRD (Fig. 3.8). The aim was to identify the phase compositions. First, the as-milled powders were characterized. Then, XRD analysis was performed for the as-synthesized powder to investigate if there was any reaction between the constituent powders during milling. After that, the combustion products

were investigated. To do so, the product pellet was crushed and the obtained powder was characterized. The goal was to identify different phases that were formed during combustion as well as to see if there was any unreacted Mo phase − an extremely desired phase in the product for better mechanical properties.

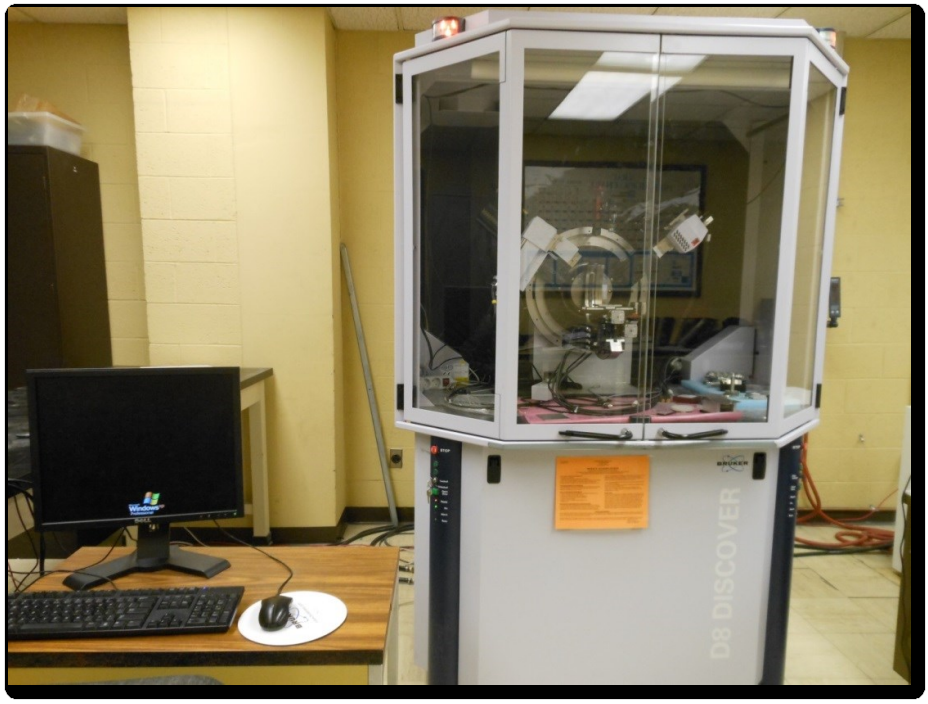

Figure 3.8: Experimental setup for XRD analysis.

3.4.2 Scanning Electron Microscopy Analysis

The particle size and morphology of the powders were characterized by scanning electron microscopy (Hitachi S-4800) (Fig. 3.9). Initially, the powders before and after milling were investigated to learn about the effect of mechanical activation (high energy ball milling). Then the product was crushed and the obtained powder was characterized to see the structure of the particles.

Figure 3.9: Experimental setup for SEM analysis.

3.4.3 Compression Test

To determine the strength of SHS compaction products, a compression test was performed using INSTRON 5866 testing machine (Fig. 3.10) in accordance with ASTM standard C773.

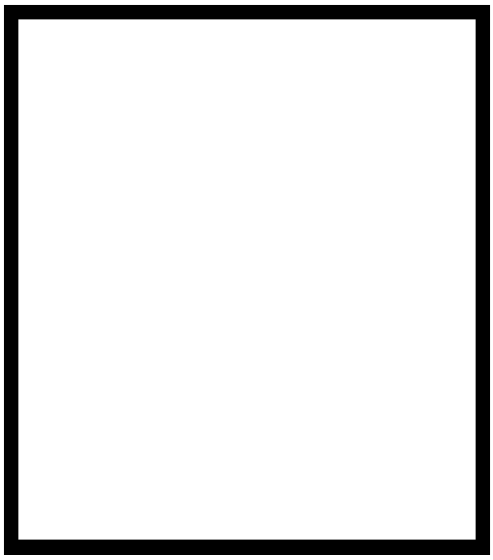

Figure 3.10: Fatigue test machine (Instron 8801).

The sample had a height of 18.4 mm. A rate of 5 mm/min was used for the displacement of the top fixture. The load-strain curve of the test was investigated, from which the compressive strength of the product was calculated.

3.4.4 Thermogravimetric Analysis

A thermogravimetric analyzer (Netzsch TGA 209 F1 Iris) was used to study the oxidation resistance of the obtained materials obtained by two methods: SHS in argon environment and SHS compaction. A sample mass of about 20 mg was taken in an alumina crucibles, the diameter of which was 5.85 mm. The samples were heated in oxygen-argon environment. 20% O_2 and 80% Ar was selected as the environment. The heating rate was 10 °C/min. The flow rates of oxygen and argon were 6 mL/min and 24 mL/min, respectively.

Figure 3.11: Thermogravimetric analyzer (Netzsch TGA 209 F1 Iris).

Chapter 4: Fabrication and Characterization of $MoSi_2$-Mo_5Si_3 Composites

4.1 Effect of Mechanical Activation

SHS experiments were conducted in argon environment. Both the milled and unmilled powders were tested. In the experiments, it was possible to ignite 12.7-mm-diameter pellets without mechanical activation. The experiments, however, revealed a remarkable effect of mechanical activation on the velocity of the combustion front propagation: it increased from 2 mm/s to about 13 mm/s.

Figures 4.1and 4.2 show the images of combustion front propagation over Mo/Si mixture. Figure 4.1 represents combustion without mechanical activation, whereas Fig 4.2 with mechanically activated powders. It is clear from the images that mechanical activation improved the reaction kinetics of the mixture and led to a faster and easier ignition. Apparently, mechanical activation reduced the particle size and increased the contact surface area between the constituent powders, thus facilitated ignition.

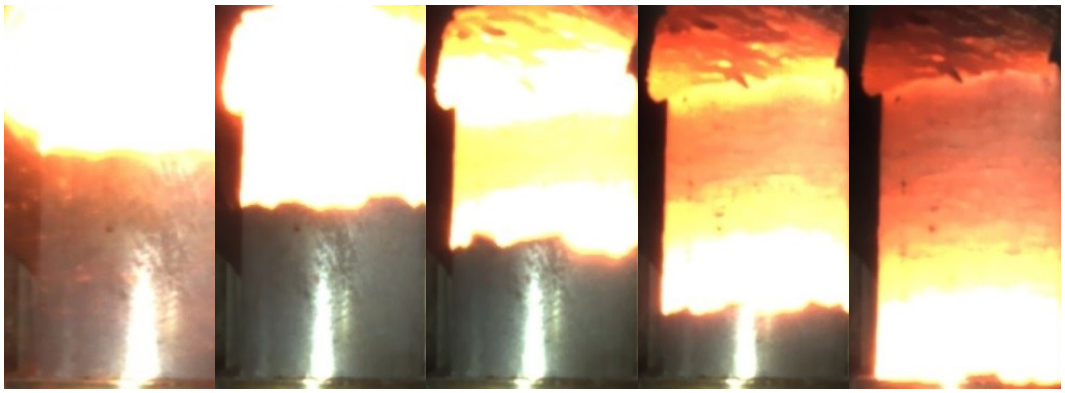

0 s 3 s 6 s 9 s 12 s

Figure 4.1: Propagation of combustion front over unmilled mixture. Time zero selected arbitrarily.

Figure 4.2: Propagation of combustion front over milled mixture. Time zero selected arbitrarily.

4.2 COMBUSTION CHARACTERISTICS

The maximum temperatures generated during combustion were recorded. Three experiments were conducted for each composition. It was observed that the average maximum temperature varied from about 1235°C to 1362°C (See Table 4.1). The temperature decreased with increasing the concentration of Mo in the mixture, which corresponds to increasing T_2 phase in the products. In addition, Table 1 shows the average combustion front velocities that were determined using the recorded videos. For clarity, the same data are also shown in Figs. 4.3 and 4.4.

Table 4.1: Compositions and combustion characteristics of the tested Mo−Si mixtures.

No.	Expected product composition		Combustion front velocity,	Maximum temperature,
	$MoSi_2$	Mo_5Si_3		
	vol%	vol%	mm/s	° C
1	100	0	5.23 ± 0.23	1259 ± 14
2	90	10	6.83 ± 0.66	1362 ± 103
3	80	20	7.67 ± 2.89	1368 ± 163
4	70	30	6.71 ± 1.81	1244 ± 38
5	60	40	5.59 ± 0.84	1235 ± 179

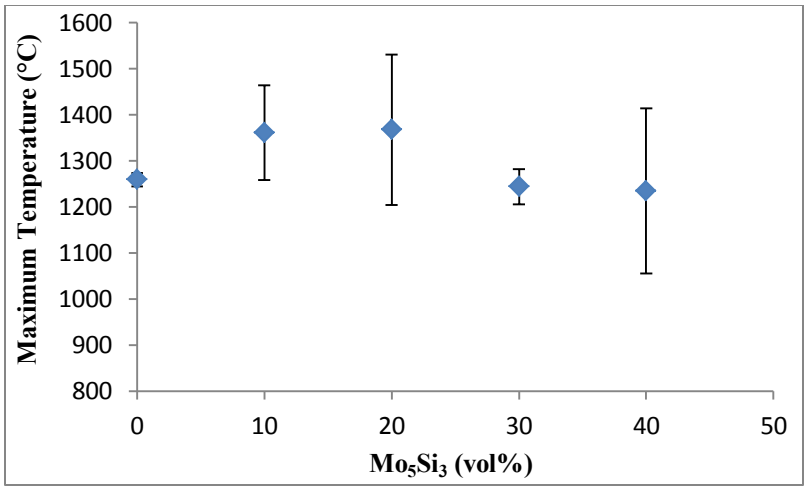

Figure 4.3: Maximum combustion temperature.

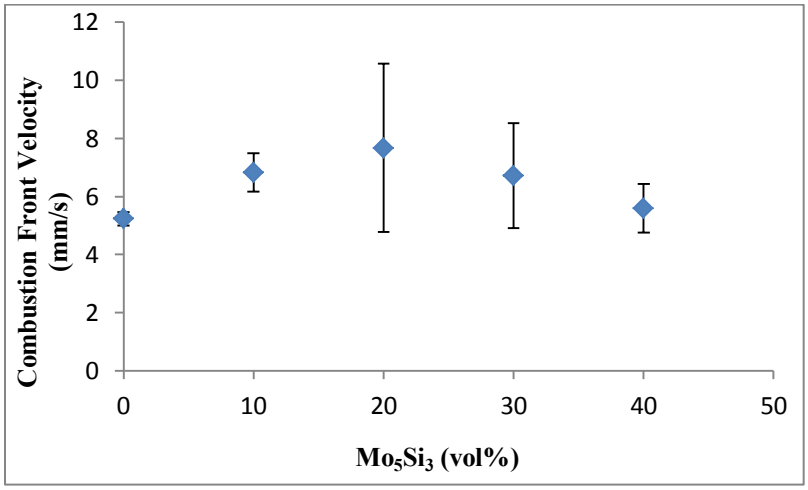

Figure 4.4: Combustion front velocity.

It can be concluded that the combustion characteristics of the tested mixtures are not strongly dependent on the concentration of T_1 phase in the products. The increase in the concentration to 50 vol% leads to a significant drop in the combustion temperature and front velocity and makes the mixture non-combustible.

4.3 X-RAY DIFFRACTION ANALYSIS

The powder after milling has been investigated with XRD analysis to see that if there was any reaction between Mo and Si during milling. Also, the combustion product was analyzed. The results are shown in Figs, 4.5 and 4.6. It is seen that the as-milled powder consists of Mo and Si. As there was no formation of $MoSi_2$ or Mo_5Si_3, it can be concluded that no reaction occurred during milling. XRD pattern of the combustion product shows that $MoSi_2$ is the major phase and Mo_5Si_3 is the secondary phase of the composite. No unreacted molybdenum or silicon was detected.

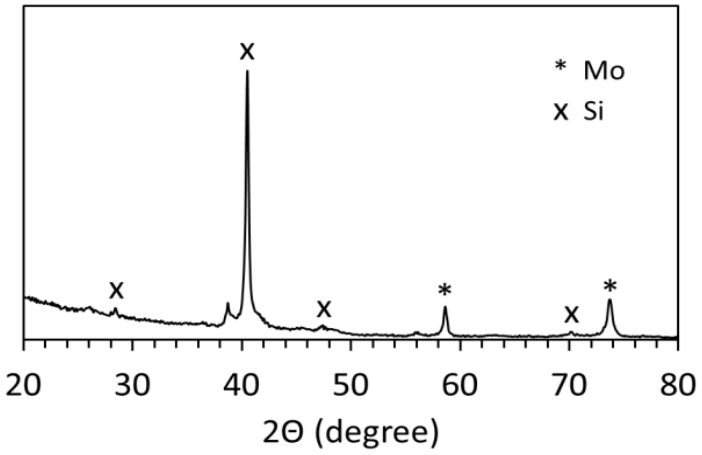

Figure 4.5: XRD pattern of Mo−Si powder of as-milled powder.

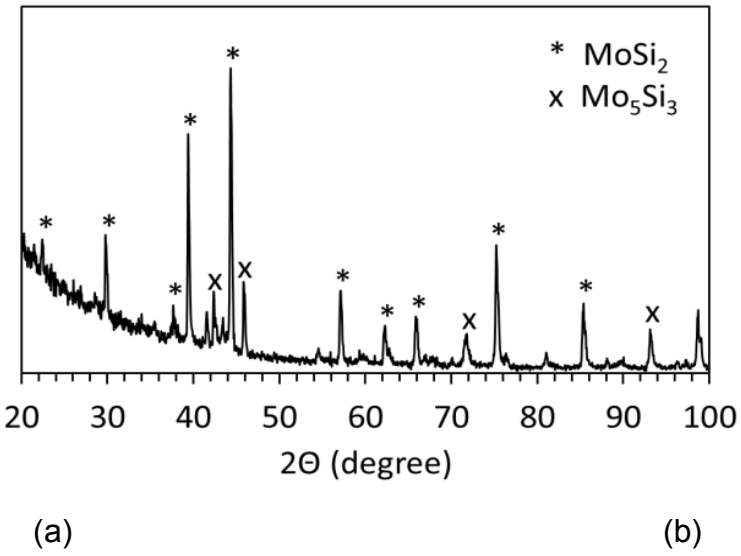

Figure 4.6: XRD pattern of Mo−Si powder of SHS products.

4.4 SCANNING ELECTRON MICROSCOPY ANALYSIS

As mentioned above, measurements with the particle size analyzer have shown that before milling Mo has the volume mean diameter of 16.64 μm and median diameter of 11.25 μm, while Si has the volume mean diameter of 10.15 μm and median diameter of 7.72 μm. Figure 4.7 shows the SEM images of Mo/Si mixture before and after milling. The image analysis indicates that milling decreased the particle size from about 10 μm to the submicron range (200−500 nm). Based on the SEM observations, it can be concluded that the structure of the as-milled powder may be considered as aggregates composed of Mo and Si nanocrystals. This nanostructured Mo−Si material is easily ignited during SHS process.

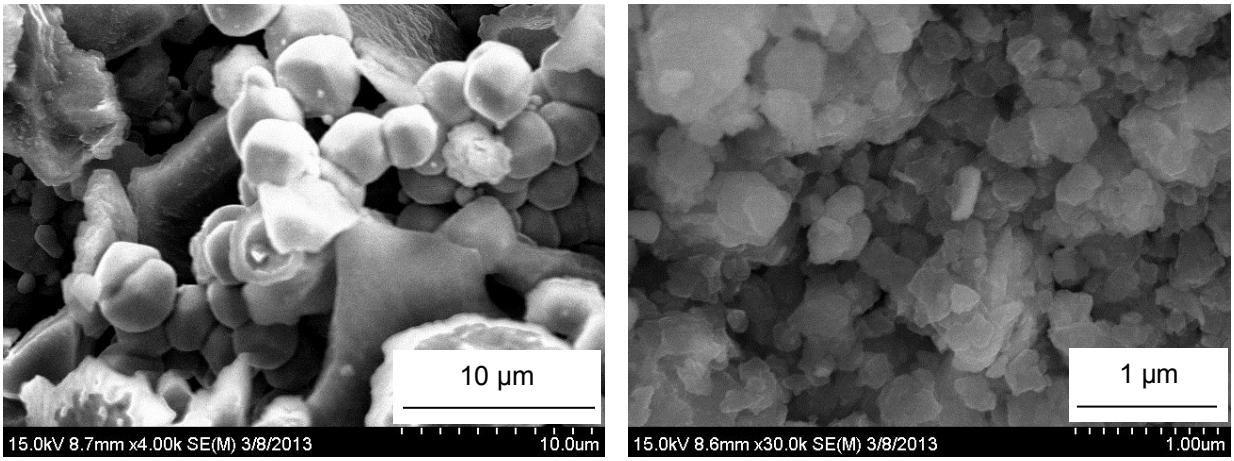

Figure 4.7: SEM micrographs of Mo−Si mixture (left) before milling and (right) after milling.

From the SEM image of the combustion products (Fig. 4.8), it is seen that most particles have a size of 0.5−1 μm; they are agglomerated and form a three-dimensional network structure.

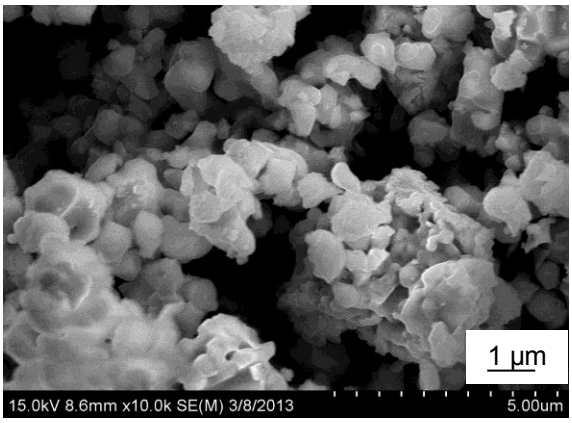

Figure 4.8: SEM micrographs of Mo−Si mixture after combustion in Argon.

4.5 SHS COMPACTION

The SHS product was investigated and it was found that the relative density was only 39% (Fig 4.9 (a)). Also, porosity was very high. So, the same composite was fabricated by SHS compaction technique. The product obtained after SHS compaction (Fig 4.9 (b)) had a lower porosity and was significantly denser than that obtained after combustion in argon. Specifically, SHS compaction products exhibited an increase in density of 55−60% as compared to non-compacted products. The volume decreased due to decreasing the length, while the diameter remained almost the same as before the compaction. The XRD pattern obtained after SHS compaction was similar to that obtained by combustion in argon.

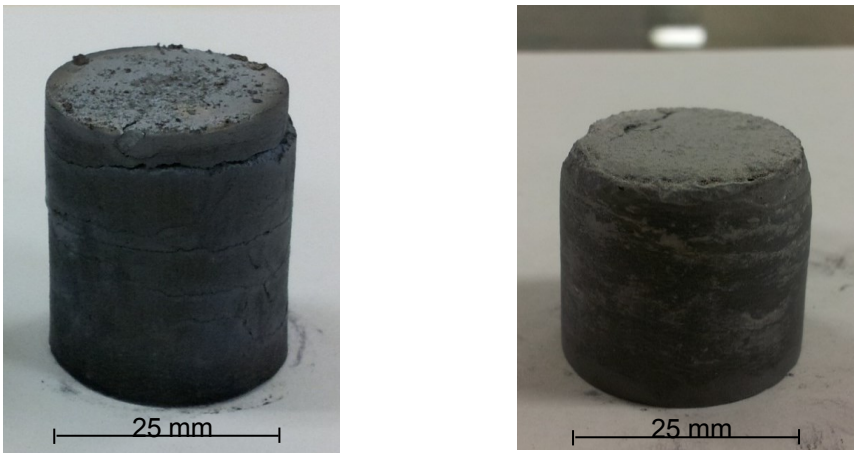

(a) (b)

Figure 4.9: Products (a) after combustion in Ar (b) after SHS compaction.

4.6 COMPRESSION TEST

The SHS compaction product (diameter 25 mm; height 17 mm) was subjected to the compression test. The displacement rate of the top fixture was equal to 5 mm/min. During the test, when the load reached 37.9 kN, the product started to break (see the load-strain curve in Fig. 4.10). Based on the test results, compressive strength was determined to be 79 MPa.

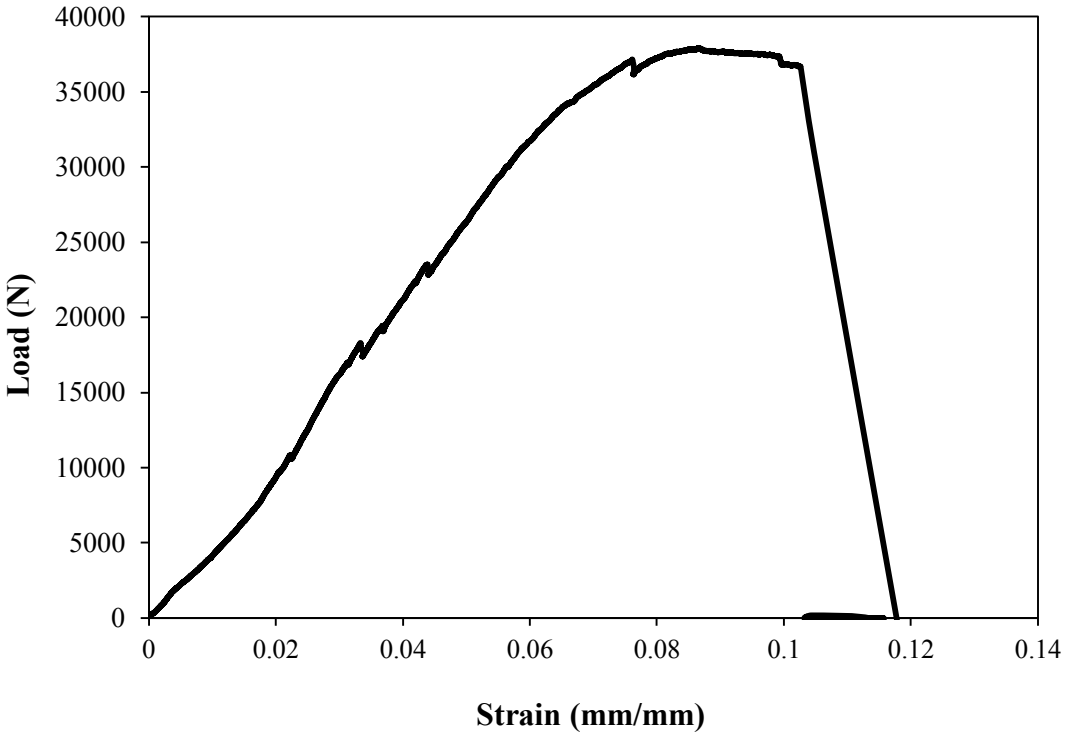

Figure 4.10: Compressive load-strain curve of the SHS compaction product.

4.7 THERMOGRAVIMETRIC ANALYSIS

Oxidation of the materials obtained by combustion in argon and by SHS compaction was studied using thermogravimetric analysis. The samples (mass: about 20 mg) in alumina crucibles (diameter: 5.85 mm) were heated in oxygen-argon (20% O_2) environment at a heating rate of 10 °C/min. The flow rates of oxygen and argon were 6 mL/min and 24 mL/min, respectively. Figure 4.11 shows the thermogravimtetric (TG) curves for the products obtained by combustion in argon and by SHS compaction.

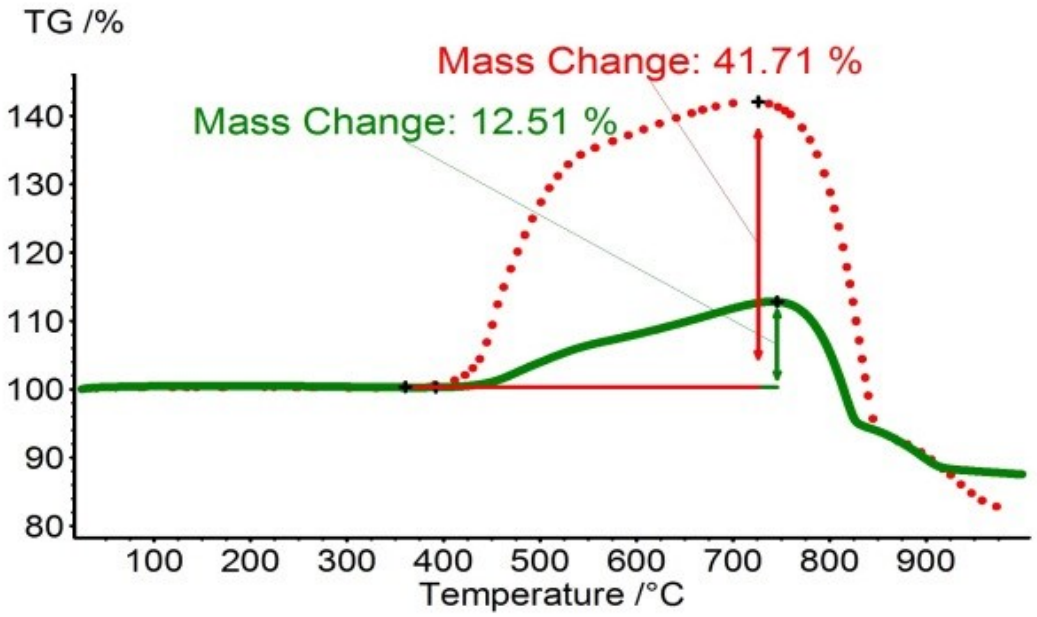

Figure 4.11: TG curves for the oxidation of $MoSi_2$–Mo_5Si_3 materials obtained by combustion in Ar (dotted lines) and by SHS compaction (solid lines).

It is seen that qualitatively the two TG curves are similar. In both cases, the mass increase due to oxidation started at about 400 °C and reached the maximum at 720–750 °C. Further increase in the temperature led to dramatic loss of mass. Note that the mass loss during oxidation of Mo-rich silicides at temperatures over 700 °C is well known in the literature [1, 13-16]; it is explained by volatilization of MoO_3 phase formed in the temperature range from 400 to 700 °C. Comparison of the two TG curves clearly shows that the use of SHS compaction significantly improves the oxidation resistance of $MoSi_2$–Mo_5Si_3 materials obtained by combustion synthesis. This effect is apparently associated with the lower porosity of SHS compaction products, which inhibits transport of oxygen to the inner surface of the obtained porous sample. It is expected that an increase in pressure during SHS compaction will further improve the oxidation resistance of the obtained $MoSi_2$–Mo_5Si_3 materials.

Chapter 5: Fabrication and Characterization of Materials Based On Mo_5SiB_2 Phase

5.1 SHS OF Mo_5SiB_2-MoB COMPOSITES

The attempts to ignite (in argon) a mechanically activated mixture of Mo, Si, and B that corresponds to Mo_5SiB_2 phase were unsuccessful. To increase the exothermicity, the composition of the initial mixture was designed according to the stoichiometry of reactions that produce two phases: Mo_5SiB_2 and MoB. The idea of adding more boron is based on the higher exothermicity of Mo−B mixture: the adiabatic flame temperature of Mo−B equimolar mixture is equal to 2310 K (calculated at 1 atm using THERMO software [20]), i.e., by about 400 K higher than for Mo−Si (1:2 mole ratio) mixture. Table 5.1 shows the compositions of the prepared mixtures and of the expected products.

Table 5.1: Compositions and combustion characteristics of the tested Mo−Si−B mixtures.

No.	**Initial mixture**			**Expected product**		***u***	***z***	***f***	***n***	***v***	***u·z***
	Mo	**Si**	**B**	**Mo_5SiB_2**	**MoB**						
	mol%	mol%	mol%	mol%	mol%	mm/s	mm	Hz		mm/s	mm^2/s
1	62.5	12.5	25	100	0	-	-	-	-	-	-
2	62.16	12.16	25.68	90	10	*	*	*	*	*	-
3	61.76	11.76	26.47	80	20	2.5	0.94	2.6	1	121	2.4
4	61.13	11.13	27.74	67	33	2.9	0.85	3.4	3	47	2.5
5	60	10	30	50	50	3.6	0.73	4.9	>3*	*	2.6
6	59.09	9.09	31.82	40	60	4.1	0.64	6.3	>3*	*	2.6
7	58.29	8.29	33.42	33	67	5.6	0.56	10.0	>3*	*	3.1

* Accurate measurements were impossible in this case.

5.1.1 Combustion Characteristics

The combustion experiments were conducted with 12.7-mm-diameter pellets in an argon environment. The results confirmed that the proposed method for increasing the mixture exothermicity works: mixture #2 (see Table 5.1) ignited and the combustion front stopped before reaching the middle of the pellet, while for mixture #3, the front traveled 90% of the pellet height and for mixtures 4–7, the front reached the bottom of the pellet. All the pellets burned in the spin combustion regime where the combustion wave propagates as the motion of one or several hot spots along a helix on the pellet surface [52-55].

For mixture 3, initially one hot spot propagated (Fig. 5.1) and after passing the middle of the pellet height, a transition to the regime with two counter-propagating spots occurred. For mixture 4, the combustion started from two counter-propagating hot spots and after three cycles transformed into the so-called three-head spin where three hot spots are moving in the same direction along a helix (Fig. 5.2). For mixtures 5−7, the number of spots was larger and they were moving rapidly along the luminous zone boundary while this zone propagated toward the bottom end of the pellet. For all the samples, a distinct trace of the spinning front remained on the product surface.

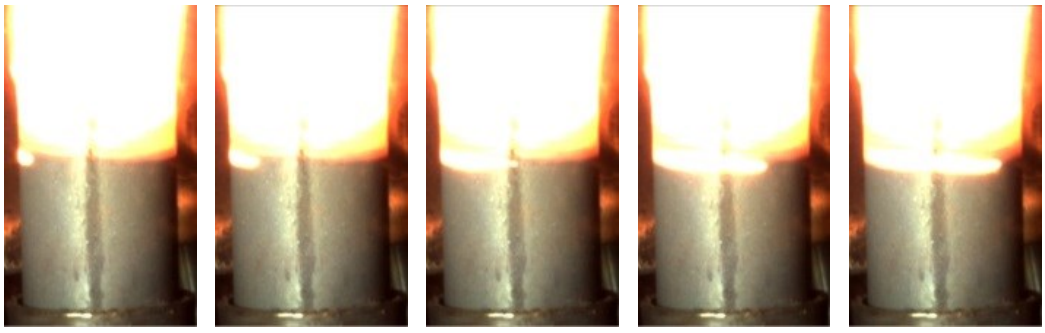

Figure 5.1: Propagation of a single spin over mixture #3 (Table 5.1) pellet. Time zero selected arbitrarily.

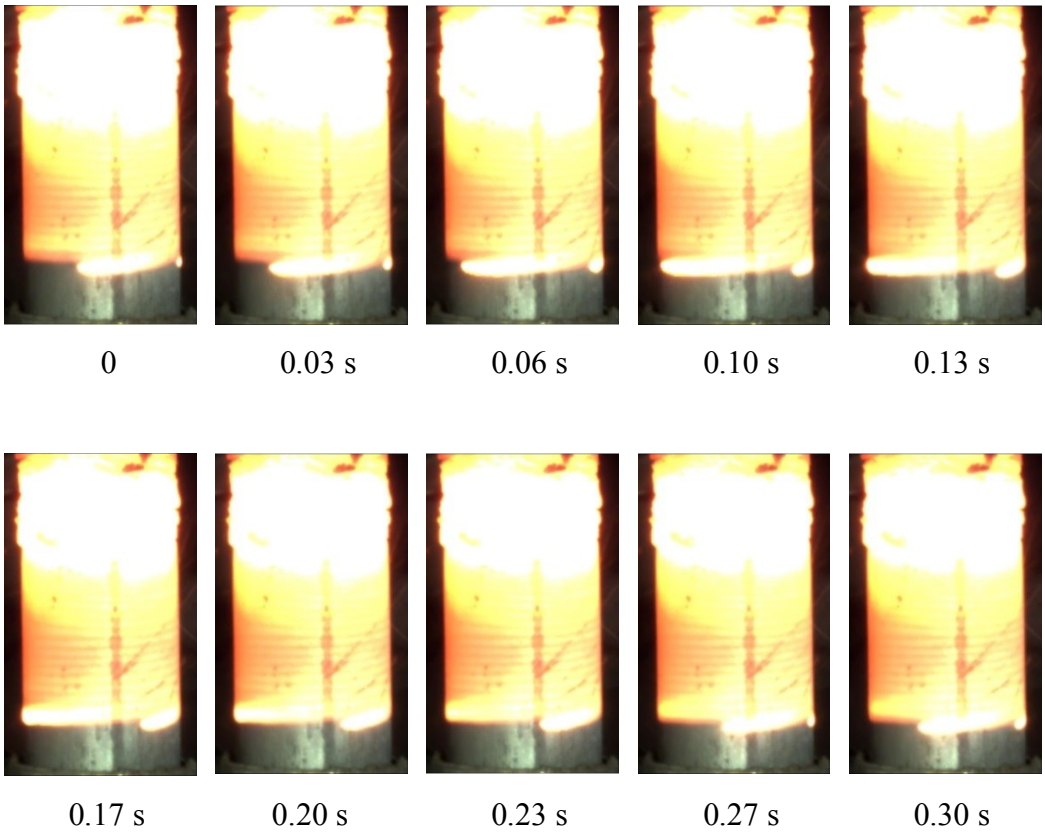

Figure 5.2: Propagation of a three-head spin over mixture #4 (Table 5.1) pellet. Time zero selected arbitrarily.

The measured characteristics of the spinning front such as the axial velocity (u), pitch (z), frequency (f), number of spin heads (n), and tangential velocity (v), are shown in Table 5.1. The pitch and frequency were measured using the trace on the product surface. Note that one of the three characteristics u, f, and z can also be calculated using the other two and an obvious relationship $u = f \cdot z$.

Different analytical and modeling approaches have been utilized to explain the spin combustion of solid systems [56-58]. A simplified theory of spin combustion developed by Novozhilov [56] predicts that the product $u \cdot z$ (or $u^2 \cdot f^{-1}$) is constant and of the same order of magnitude as the thermal diffusivity of the medium (the pitch plays a role of the preheat zone in the flame). The obtained values of $u \cdot z$ are, indeed, close to each other (see Table 5.1). It is also well known that for many powdered mixtures used in SHS, the thermal diffusivity is of the order

of 1 mm^2/s [59, 60] so that the obtained values of $u \cdot z$ are of the same order of magnitude as the thermal diffusivity. In addition, the measured values of the tangential velocity v for mixtures 3 and 4 (121 and 47 mm/s, respectively) correlate with the values 106 and 45 mm/s, respectively, obtained using the mass conservation equation: $v = \pi \cdot d \cdot u \cdot n^{-1} \cdot z^{-1}$, where d is the pellet diameter. Thus, the obtained characteristics of spin combustion are in good agreement with Novozhilov's theory.

Thermocouple measurements have shown that in any of the tested Mo-Si-B mixtures the maximum temperature did not reach the melting point of Si, 1414 °C (the melting points of Mo and B are much higher). Thus, the reaction mechanism during the observed spin combustion was based on solid-phase diffusion, with no liquid involved. Also, the temperature profiles contained a single maximum, indicating that the reactions occurred simultaneously.

5.1.2 X-ray Diffraction Analysis

X-ray diffraction analysis of the combustion products has shown that in each experiment, the obtained composition was not a binary (Mo_5SiB_2–MoB) mixture. Figure 5.3 shows an XRD pattern for mixture #4. The composition includes Mo_5SiB_2, MoB, $MoSi_2$, Mo_5Si_3, Mo_2B, and Mo. It is possible that the product also contains B, which cannot be seen in the pattern because amorphous boron was used in the experiments. It is seen that Mo_5SiB_2 and Mo exhibit the highest peaks and MoB is apparently the third major component. XRD patterns obtained for mixtures 5, 6, and 7 are similar (figs 5.4, 5.5, and 5.6), but they report an important trend: the Mo-to-Mo_5SiB_2 intensity ratio, determined using the highest peaks for each phase, is equal to 1.39, 1.18, 0.75, and 0.62 for mixtures 4, 5, 6, and 7, respectively. Thus, with increasing the content of MoB in the product composition, the content of Mo phase decreases.

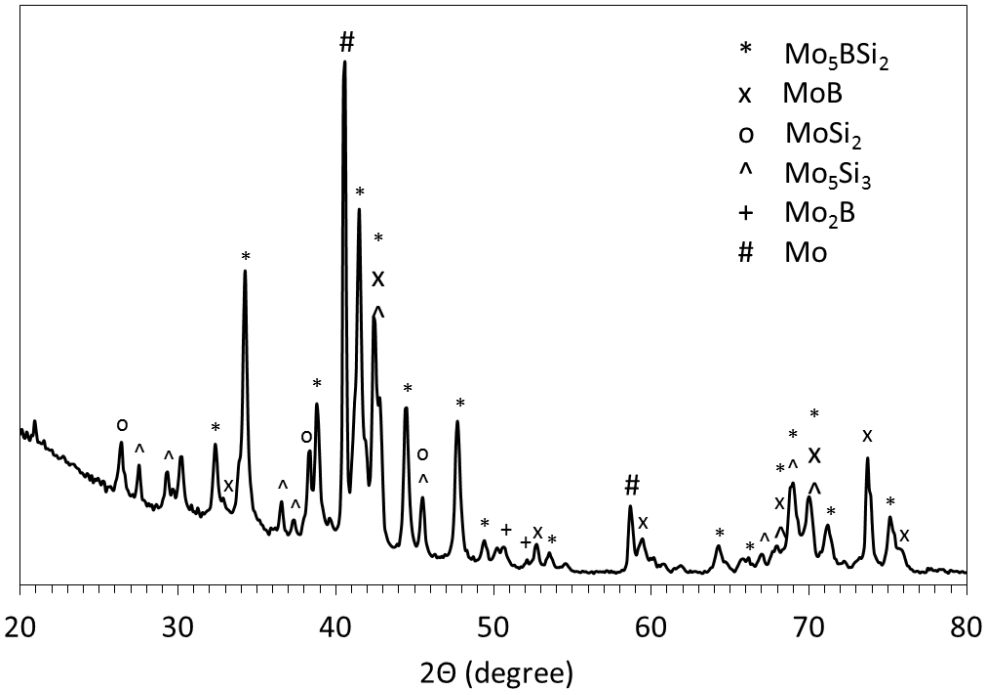

Figure 5.3: XRD pattern of products obtained by combustion of Mo−Si−B mixture #4 (Table 5.1).

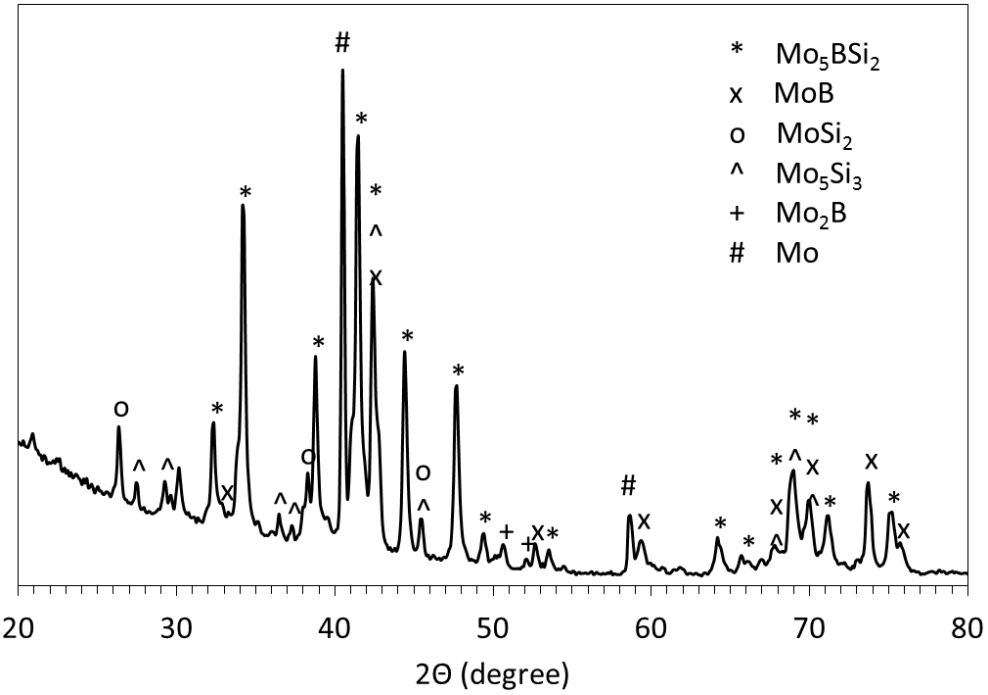

Figure 5.4: XRD pattern of products obtained by combustion of Mo−Si−B mixture #5 (Table 5.1).

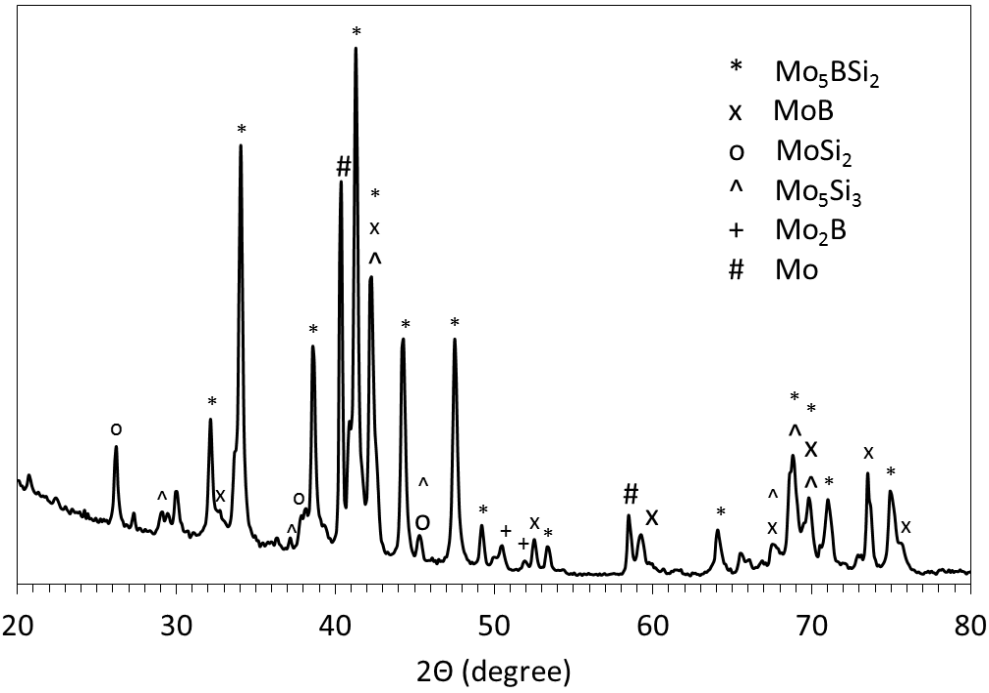

Figure 5.5: XRD pattern of products obtained by combustion of Mo−Si−B mixture #6 (Table 5.1).

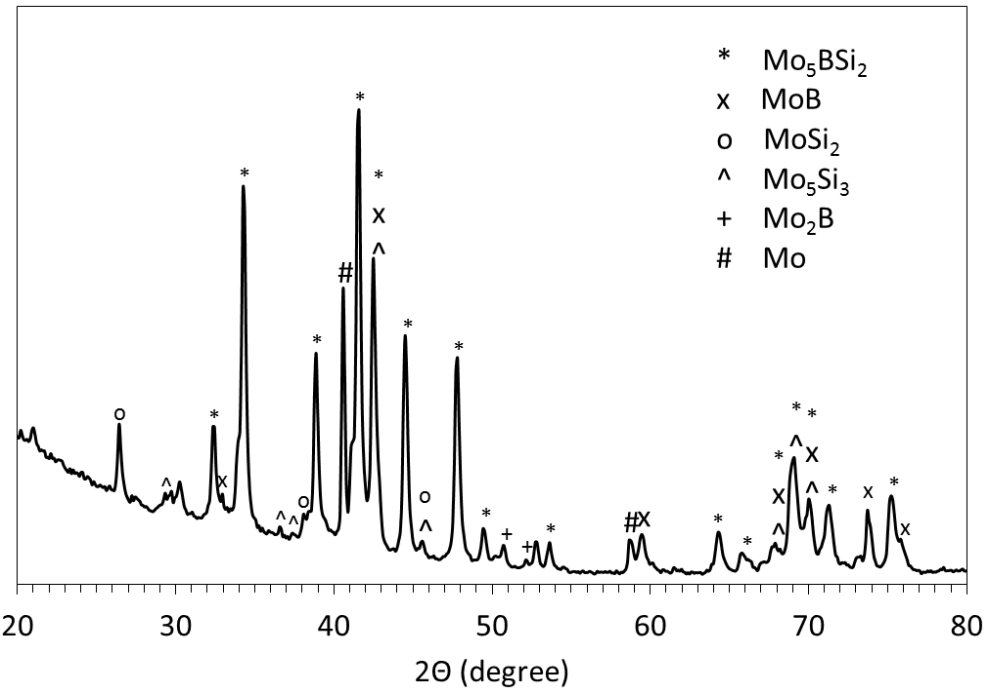

Figure 5.6: XRD pattern of products obtained by combustion of Mo−Si−B mixture #7 (Table 5.1).

5.1.3 Thermogravimetric Analysis

It is well known that increasing the amount of Mo phase improves mechanical properties of molybdenum silicides and borosilicides, but decreases the oxidation resistance because of the formation and volatilization of MoO_3 [1, 13-17]. To determine the effect of Mo phase on the oxidation resistance of the obtained materials, mixtures 3, 4, and 7 were subjected to thermogravimetric analysis in oxygen−argon flow. The flow rate and the heating rate were the same as in the aforementioned tests of $MoSi_2$−Mo_5Si_3 composites. For all the samples, the TG and calculated differential thermal analysis (c-DTA) curves were virtually identical (Figs. 5.7, 5.8, and 5.9). The mass increases are 54.5%, 54.8, and 54.2% for mixtures 3, 4, and 7 respectively. Thus, it can be concluded that oxidation resistance of the obtained Mo−Si−B materials is independent on the concentration of Mo phase in the products so that the materials with higher Mo contents are preferable because of better mechanical properties. The oxidation resistance of these materials could be improved by using SHS compaction as shown in Section 4.1.5.

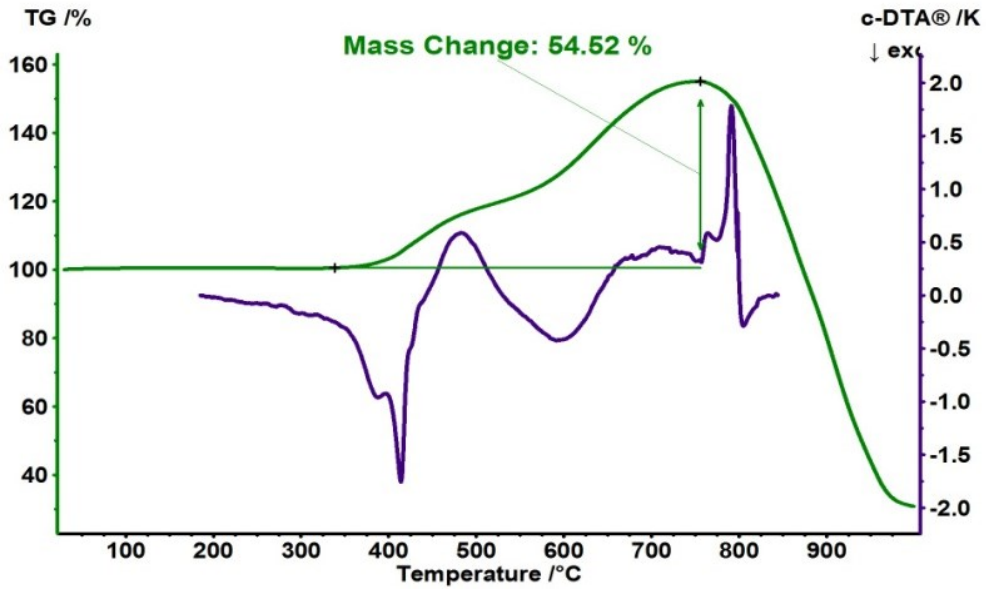

Figure 5.7: TG and c-DTA curves for the oxidation of the product obtained by combustion of Mo−Si−B mixture #3 (Table 5.1).

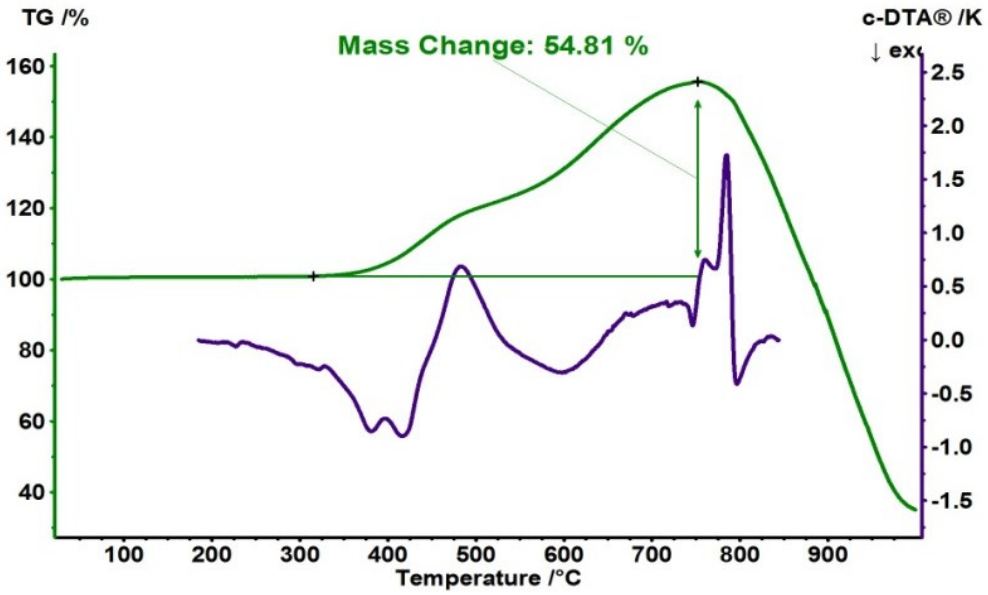

Figure 5.8: TG and c-DTA curves for the oxidation of the product obtained by combustion of Mo−Si−B mixture #4 (Table 5.1).

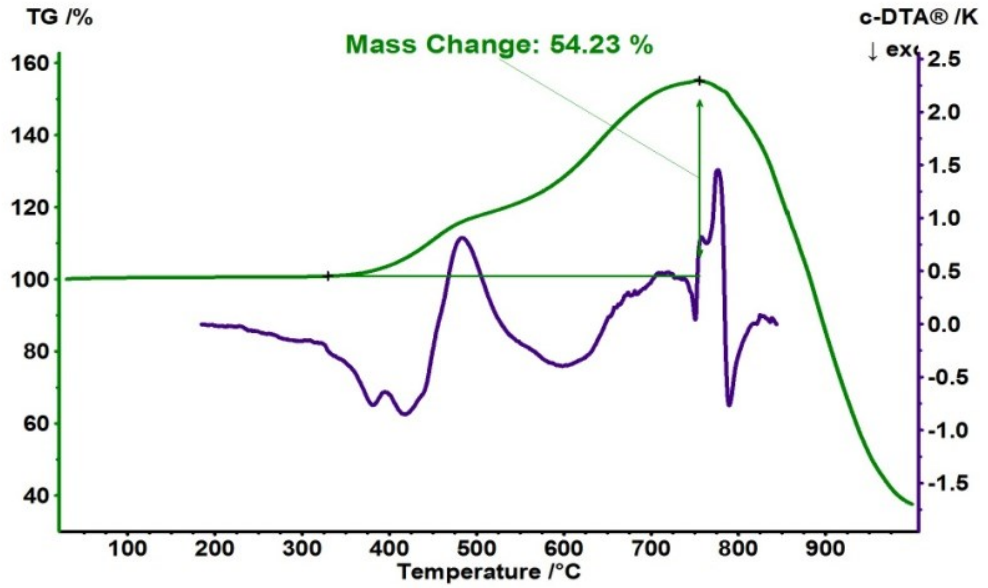

Figure 5.9: TG and c-DTA curves for the oxidation of the product obtained by combustion of Mo−Si−B mixture #7 (Table 5.1).

5.2 COMBUSTION SYNTHESIS OF A SINGLE Mo_5SiB_2 (T_2) PHASE

To fabricate a single T_2 phase, we used the "chemical oven" technique. Both milled and unmilled powders were tested. We prepared composite pellets that included a core of Mo-Si-B (5:1:2 mole ratio) mixture inside a shell made of Ti/B (1:2 mole ratio) mixture. The highly-exothermic Ti/B mixture was used as a source of additional heat to enable ignition of the core. To make the composite pellet, first, Mo-Si-B mixture was compacted into a pellet (diameter: 13 mm, height: 15-20 mm). Then this pellet was submerged into Ti/B mixture inside a 25-mm die and pressed again. The resulting composite pellet is shown in Fig. 5.10. This pellet was ignited in an argon environment at 1 atm.

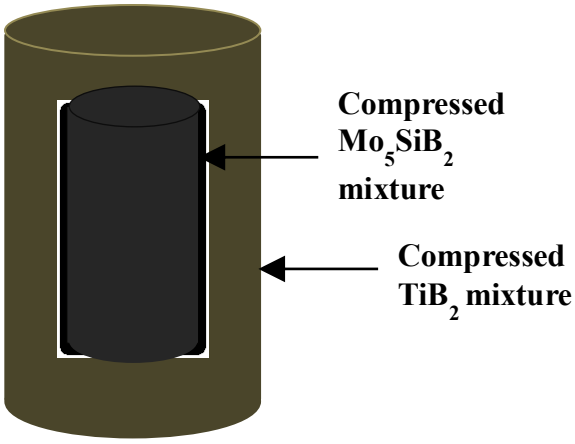

Figure 5.10: Composite pellet for chemical oven experiments.

5.2.1 SHS products

Figure 5.11 shows photographs of the combustion products. The product in the left image was obtained by combustion of the unmilled powder mixture, while the right image shows the product obtained from the milled (mechanically activated) powder. Although the product in the right image looks more metallic and less porous than the left one, it had large cracks throughout.

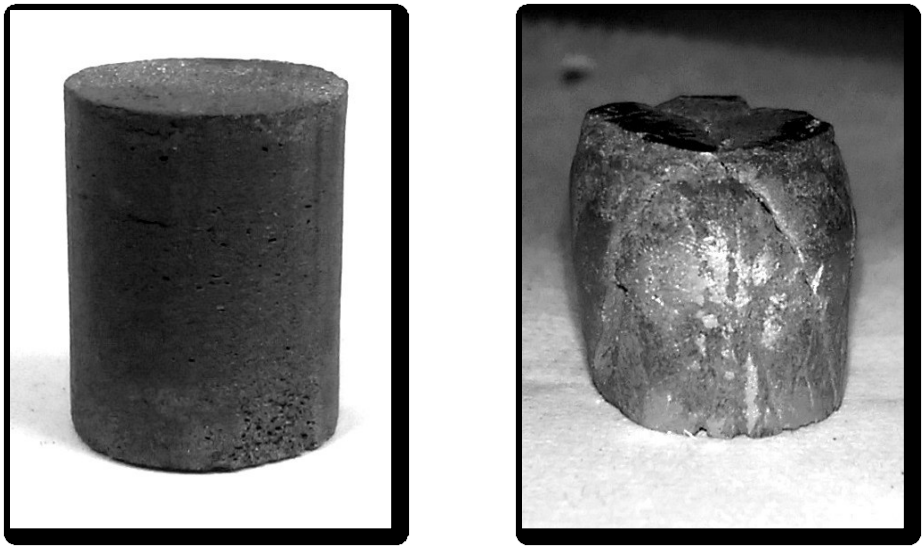

Figure 5.11: Combustion Products (left) without and (right) with mechanical activation.

5.2.2 X-ray Diffraction Analysis

XRD patterns of both products are shown in Figs. 5.12 and 5.13. These patterns are quite similar. They confirm the abundance of Mo_5SiB_2 phase in each sample. Small peaks of Mo and Mo_3Si are also observed.

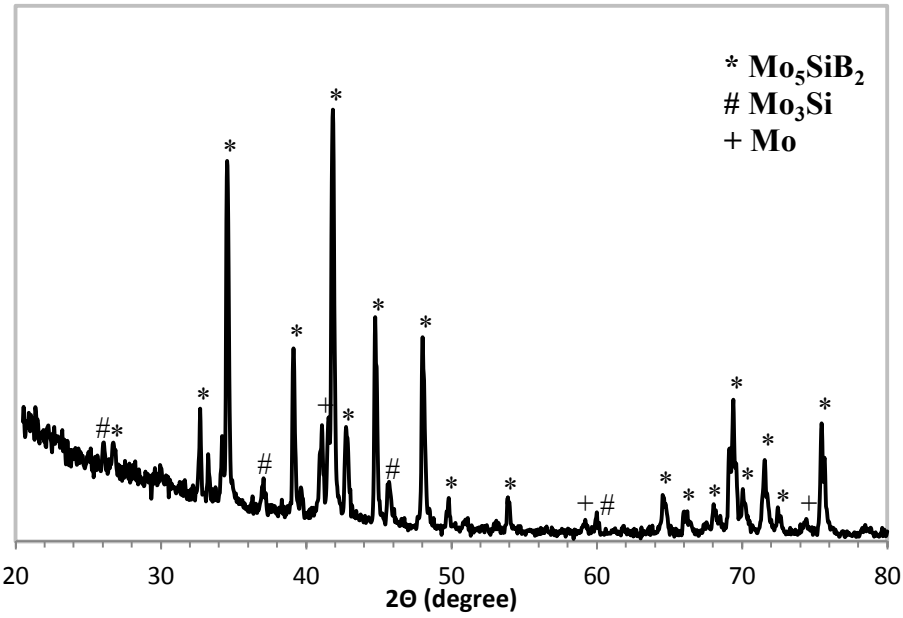

Figure 5.12: XRD pattern of products obtained by chemical oven SHS of unmilled mixture.

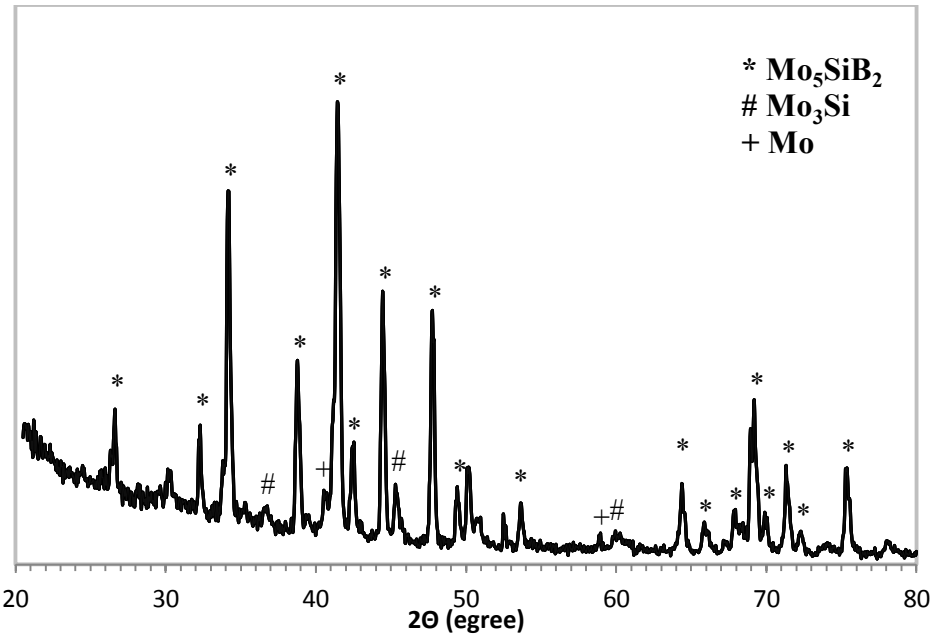

Figure 5.13: XRD pattern of products obtained by chemical oven SHS of milled mixture.

5.2.3 Scanning Electron Microscopy Analysis

The powder before and after milling (Fig. 5.14) were analyzed in SEM that shows the particle distribution and confirms the reduction of particle size by milling.

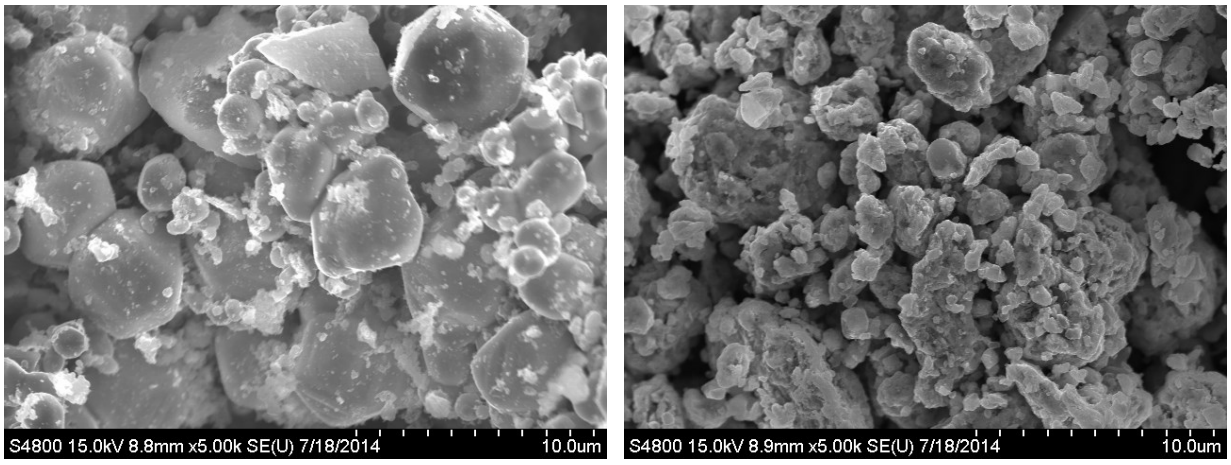

Figure 5.14: SEM micrograph of Mo−Si−B mixture (left) before milling and (right) after milling.

Also, the combustion product was analyzed in SEM. Figure 5.15 shows the SEM image of the combustion product obtained from unmilled powder, while the SEM image of the product obtained from the milled powder is shown in figure 5.16.

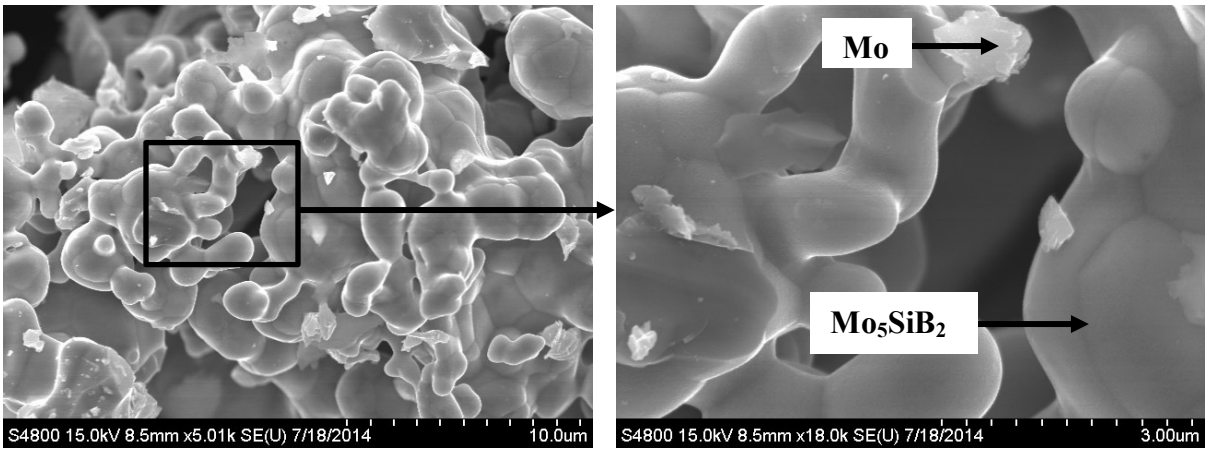

Figure 5.15: SEM micrograph of Mo−Si−B mixture after chemical oven combustion synthesis with unmilled powder.

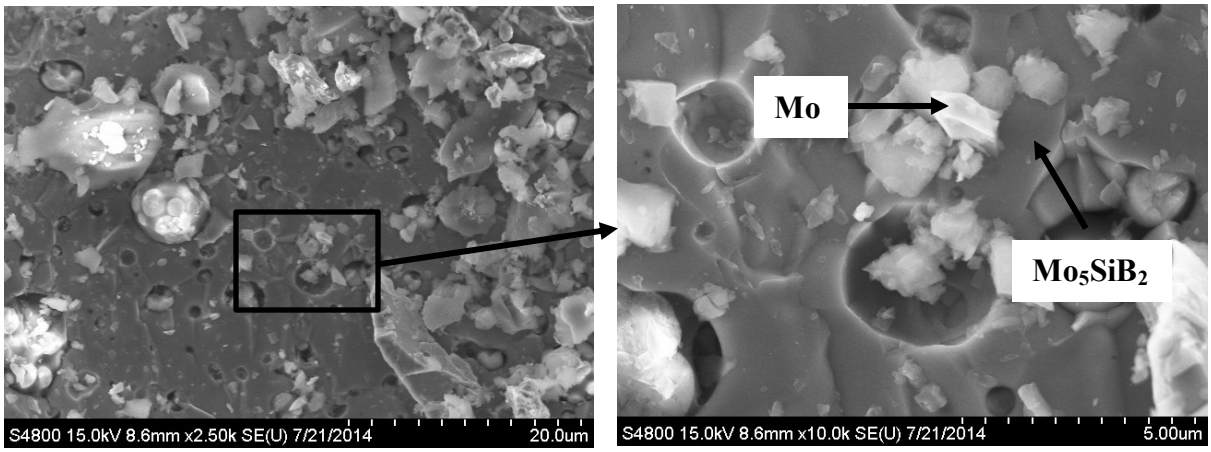

Figure 5.16: SEM micrograph of Mo−Si−B mixture after chemical oven combustion synthesis with milled powder.

Due to some limitation to obtain electron backscatter (BSE) images, these micrographs have been compared with the results of other researchers to identify the phase contents. Two such results are shown in Fig. 5.17.

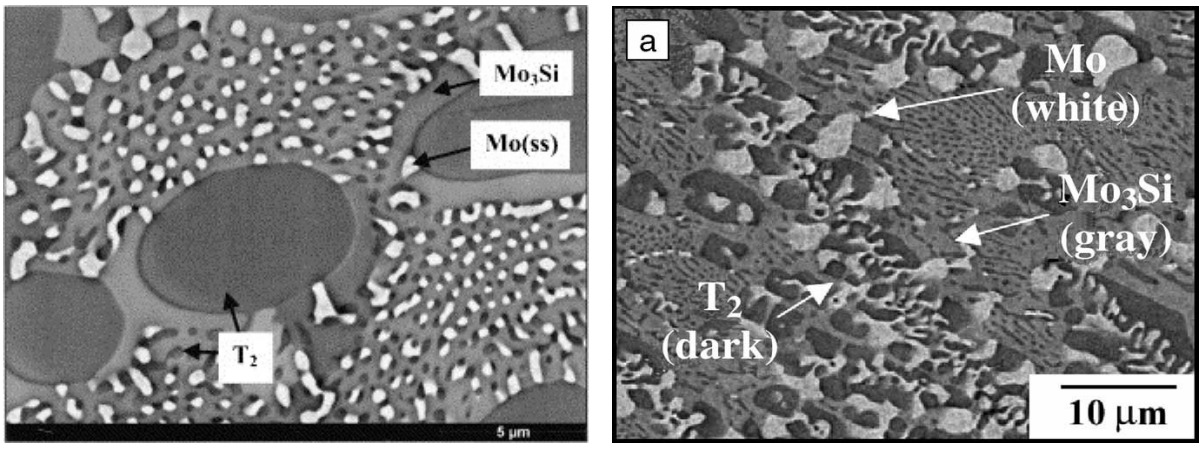

Figure 5.17: Backscattered electron image of (left) as-cast Mo–13Si–15B alloy [61] and (right) as-cast Mo-14.2Si-9.6B alloy [62].

Comparing with the aforementioned images, it can be inferred that the resulting microstructures consisted of Mo particles distributed throughout a network of the intermetallic phases Mo_3Si and Mo_5SiB_2. Bright grains in the micrograph correspond to α-Mo phase. Due to its higher average atomic number, molybdenum appears lighter than the intermetallic phases. It is difficult to distinguish T_2 and Mo_3Si phases. The presence of molybdenum particles improves the mechanical properties of the material. However, it is experimentally proved that for significant improvement, these alloys need to be processed in such a way that molybdenum is present as a continuous network.

5.2.4 Compression Test

The compressive strength of the product obtained by chemical oven combustion synthesis with the unmilled powder was investigated using the fatigue test machine. Same ASTM standard and displacement rate was maintained as described in chapter 4. Three different combustion

products were tested and the maximum compressive strength was found as 53 MPa. Figure 5.18 shows the obtained stress-strain curves.

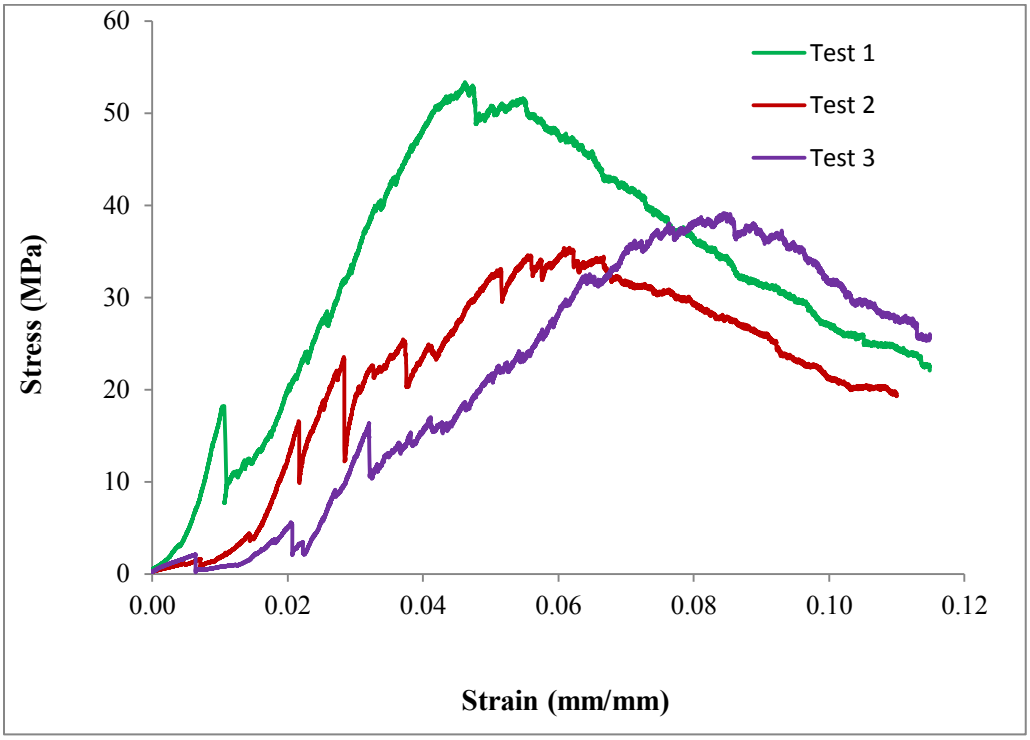

Figure: 5.18: Stress-strain curves obtained in three tests.

Chapter 6: Conclusion

$MoSi_2$−Mo_5Si_3 composites and materials based on Mo_5SiB_2 phase have been obtained by mechanically activated SHS. It has been shown that use of SHS compaction (quasi-isostatic pressing) significantly improved oxidation resistance of the obtained $MoSi_2$−Mo_5Si_3 composites. Also, it increased the product density by over 50% as compared to the product obtained by SHS in argon. The compressive strength of the product was also significantly improved.

Combustion of Mo−Si−B mixtures for the formation of Mo_5SiB_2 phase becomes possible if the composition is designed for the addition of reactions leading to the formation of molybdenum boride. These mixtures exhibit spin combustion, the characteristics of which are in good agreement with the spin combustion theory.

Oxidation resistance of the obtained Mo−Si−B materials is independent on the concentration of Mo phase in the products so that the materials with a higher Mo content are preferable because of better mechanical properties.

Chemical oven combustion synthesis technique can be used to fabricate Mo_5SiB_2 and Mo_5SiB_2- based materials. However, to obtain better mechanical properties, it is necessary to select compositions and experimental parameters in such a way that the intermetallic phases Mo_5SiB_2 and Mo_3Si are distributed uniformly in the continuous network of α-Mo.

References

[1] J. H. Perepezko, "The Hotter the Engine, the Better," *Science,* vol. 326, pp. 1068-1069, 2009.

[2] J. J. Petrovic, "Mechanical behavior of $MoSi_2$ and $MoSi_2$-composites," *Materials Science and Engineering: A 192–193, Part 1,* pp. 31-37, 1995.

[3] A. K. Vasudévan and J. J. Petrovic, "A comparative overview of molybdenum disilicide composites," *Materials Science and Engineering: A 155,* pp. 1-17, 1992.

[4] R. B. Schwarz, S. R. Srinivasan, J. J. Petrovic and C. J. Maggiore, "Synthesis of molybdenum disilicide by mechanical alloying," *Materials Science and Engineering: A 155,* pp. 75-83, 1992.

[5] R. Gibala, A. K. Ghosh, D. C. Van Aken, D. J. Srolovitz, A. Basu, H. Chang, D. P. Mason and W. Yang, "Mechanical behavior and interface design of $MoSi_2$-based alloys and composites," *Materials Science and Engineering: A 155,* pp. 147-158, 1992.

[6] Z. Yao, J. Stiglich and T. S. Sudarshan, "Molybdenum silicide based materials and their properties," *Journal of Materials Engineering and Performance,* vol. 8, pp. 291-304, 1999.

[7] K. Sadananda, C. R. Feng, R. Mitra and S. C. Deevi, "Creep and fatigue properties of high temperature silicides and their composites," *Materials Science and Engineering: A 261,* pp. 223-238, 1999.

[8] J. J. Petrovic and A. K. Vasudevan, "Key developments in high temperature structural silicides," *Materials Science and Engineering: A 261,* pp. 1-5, 1999.

[9] J. J. Petrovic, "Toughening strategies for $MoSi_2$-based high temperature structural silicides," *Intermetallics 8,* pp. 1175-1182, 2000.

[10] J. Subrahmanyam and R. M. Rao, "Combustion synthesis of $MoSi_2$-WSi_2 alloys," *Materials Science and Engineering: A 183,* pp. 205-210, 1994.

[11] H. Zhang, P. Chen, J. Yan and S. Tang, "Fabrication and wear characteristics of $MoSi_2$ matrix composite reinforced by WSi_2 and La_2O_3," *International Journal of Refractory Metals and Hard Materials 22(6),* pp. 271-275, 2004.

[12] Y. -. Jeng and E. J. Lavernia, "Processing of molybdenum disilicide," *Journal of Materials Science,* vol. 29, pp. 2557-2571, 1994.

[13] H. Nowotny, E. Dimakopoulou, and H. Kudielka, "Untersuchungen in den Dreistoffsystemen: Molybdän-Silizium-Bor, Wolfram-Silizium-Bor und in dem System: VSi_2-$TaSi_2$," *Mh. Chem.,* vol. 88, pp. 180-192, 1957.

[14] D. M. Dimiduk and J. H. Perepezko, "Mo-Si-B Alloys: Developing a Revolutionary Turbine-Engine Material," *MRS Bulletin,* vol. 28, pp. 639-645, 2003.

[15] D. M. Berczik, "Method for enhancing the oxidation resistance of a molybdenum alloy, and a method of making a molybdenum alloy, *United States Patent*, Patent Number 5,595, and 616, 1997.

[16] J. A. Lemberg and R. O. Ritchie, "Mo-Si-B alloys for ultrahigh-temperature structural applications," *Advanced Materials 24(26),* pp. 3445-3480, 2012.

[17] R. Mitra, "Mechanical Behavior and Oxidation Resistance of Structural Silicides," *International Materials Review,* vol. 51, pp. 13-64, 2006.

[18] K. Morsi, "The diversity of combustion synthesis processing: a review," *Journal of Materials Science,* vol. 47, pp. 68-92, 2011.

[19] Z. A. Munir and U. Anselmi-Tamburini, "Self-propagating exothermic reactions: the synthesis of high-temperature materials by combustion," *Materials Science Reports,* vol. 3, pp. 277-365, 1989.

[20] J. J. Moore and H. J. Feng, "Combustion synthesis of advanced materials: Part II. Classification, applications and modeling," *Progress in Materials Science 39(4–5),* pp. 275-316, 1995.

[21] A. A. Shiryaev, "Thermodynamics of SHS Processes: An Advanced Approach," *International Journal of Self-Propagating High-Temperature Synthesis,* vol. 4, pp. 351-362, 1995.

[22] A. R. Sarkisyan, S. K. Dolukhanyan, I. P. Borovinskaya and A. G. Merzhanov, "Laws of the combustion of mixtures of transition metals with silicon and the synthesis of silicides," *Combustion, Explosion and Shock Waves,* vol. 14, pp. 310-314, 1978.

[23] S. Zhang and Z. A. Munir, "Synthesis of molybdenum silicides by the self-propagating combustion method," *Journal of Materials Science,* vol. 26, pp. 3685-3688, 1991.

[24] J. Gao and W. Jiang, "Combustion Synthesis of Mo_5Si_3 in Chemical Furnace," *International Journal of Self-Propagating High-Temperature Synthesis,* vol. 17, pp. 49-53, 2008.

[25] C. L. Yeh and W. H. Chen, "Combustion synthesis of $MoSi_2$ and $MoSi_2$–Mo_5Si_3 composites," *Journal of Alloys and Compounds 438,* pp. 165-170, 2007.

[26] C. Gras, D. Vrel, E. Gaffet and F. Bernard, "Mechanical activation effect on the self-sustaining combustion reaction in the Mo–Si system," *Journal of Alloys and Compounds 314,* pp. 240-250, 2001.

[27] C. Gras, E. Gaffet and F. Bernard, "Combustion wave structure during the $MoSi_2$ synthesis by mechanically-activated self-propagating high-temperature synthesis (MASHS): In situ time-resolved investigations," *Intermetallics 14(5),* pp. 521-529, 2006.

[28] J. Kajuch and K. Vedula, "Advances in Powder Metallurgy," *Proceedings of the 1990 Powder Metallurgy Conference and Exhibition, Part 2.* pp. 187, 1990.

[29] N. Iwatomo and S. Uesaka, *Proceedings of the Fourth International Conference on Ceramic Powder Processing Science,* 1990, pp. 177.

[30] S. Jayashankar and M. J. Kaufman, "In-situ reinforced $MoSi_2$ composites by mechanical alloying," *Scripta Metallurgica et Materialia 26(8),* pp. 1245-1250, 1992.

[31] R. B. Schwarz, S. R. Srinivasan, J. J. Petrovic and C. J. Maggiore, "Synthesis of molybdenum disilicide by mechanical alloying," *Materials Science and Engineering: A 155,* pp. 75-83, 1992.

[32] L. H. Yu, "Shock synthesis and synthesis-assisted shock consolidation of silicides," *Journal of Materials Science,* vol. 26, pp. 601-611, 1991.

[33] S. C. Deevi, "Self-propagating high-temperature synthesis of molybdenum disilicide," *Journal of Materials Science,* vol. 26, pp. 3343-3353, 1991.

[34] A. Chrysanthou, R. C. Jenkins, M. J. Whiting and P. Tsakiropoulos, "A study of the combustion synthesis of $MoSi_2$ and $MoSi_2$-matrix composites," *Journal of Materials Science,* vol. 31, pp. 4221-4226, 1996.

[35] J. Xu, H. Li, H. Wu and F. Lei, "Preparation of $MoSi_2$/SiC composite by mechanical-assistant combustion synthesis method," *Journal of Alloys and Compounds 487,* pp. 326-330, 2009.

[36] J. Xu, H. Wu and B. Li, "Synthesis of $MoSi_2$/WSi_2 nanocrystalline powder by mechanical-assistant combustion synthesis method," *International Journal of Refractory Metals and Hard Materials 28(2),* pp. 217-220, 2010.

[37] J. Xu, B. Zhang, G. Jiang, W. Li and H. Zhuang, "Synthesis of SiC_w/$MoSi_2$ powder by the "chemical oven" self-propagating combustion method," *Ceramic International 32(6),* pp. 633-636, 2006.

[38] J. Xu, B. Zhang, G. Jiang, W. Li and L. Zhuang, "Fabrication and characterization of SiC_w/$MoSi_2$ composite from COSHSed powder," *Journal of Materials Science,* vol. 42, pp. 5795-5798, 2007.

[39] E. A. Levashov, Y. S. Pogozhev, A. Y. Potanin, N. A. Kochetov, D. Y. Kovalev, N. V. Shvyndina and T. A. Sviridova, "Self-propagating high-temperature synthesis of advanced ceramics in the Mo–Si–B system: Kinetics and mechanism of combustion and structure formation," *Ceramic International 40(5),* pp. 6541-6552, 2014.

[40] E. A. Olevsky, E. R. Strutt and M. A. Meyers, "Combustion synthesis and quasi-isostatic densification of powder cemets," *Journal of Materials Processing Technology 121(1),* pp. 157-166, 2002.

[41] Q. Xu, X. Zhang, J. Han, X. He and V. L. Kvanin, "Combustion synthesis and densification of titanium diboride–copper matrix composite," *Materials Letters 57(28),* pp. 4439-4444, 2003.

[42] A. Delgado and E. Shafirovich, "Towards better combustion of lunar regolith with magnesium," *Combustion and Flame 160(9),* pp. 1876-1882, 2013.

[43] M. M. Pacheco, R. H. B. Bouma and L. Katgerman, "Combustion synthesis of TiB_2-based cermets: modeling and experimental results," *Applied Physics A,* vol. 90, pp. 159-163, 2008.

[44] H. C. Yi and J. J. Moore, "A novel technique for producing NiTi shape memory alloy using the thermal explosion mode of combustion synthesis," *Scripta Metallurgica 22(12),* pp. 1889-1892, 1988.

[45] G. A. Adadurov, I. P. Borovinskaya, Y. A. Gordopolov and A. G. Merzhanov, "Tecnological Fundamentals of SHS Compacting," *Inzhenerno-Fizicheskii Zhurnal,* vol. 63, pp. 538-546, 1992.

[46] E. A. Olevsky, J. Ma, J. C. LaSalvia and M. A. Meyers, "Densification of porous bodies in a granular pressure-transmitting medium," *Acta Materialia 55(4),* pp. 1351-1366, 2007.

[47] Z. Xinghong, Z. Chuncheng, Q. Wei, H. Xiaodong and V. L. Kvanin, "Self-propagating high temperature combustion synthesis of TiC/TiB_2 ceramic–matrix composites," *Composites Science and Technology 62(15),* pp. 2037-2041, 2002.

[48] M. M. Pacheco, "Self-sustained High-temperature Reactions: Initiation, Propagation, Synthesis," 2007.

[49] V. L. Kvanin, N. T. Balikhina, S. G. Vadchenko, I. P. Borovinskaya and A. E. Sychev, "Preparation of ɣ-TiAl Intermetallic Compounds through Self-Propagating High-Temperature Synthesis and Compaction," *Inorganic Materials,* vol. 44, pp. 1194-1198, 2008.

[50] M. Kholghy, S. Kharatyan and H. Edris, "SHS/PHIP of ceramic composites using ilmenite concentrate," *Journal of Alloys and Compounds 502(2),* pp. 491-494, 2010.

[51] F. Zhang, Z. Fu, J. Zhang, H. Wang, W. Wang, Y. Wang and J. Shi, "Ultra-fast densification of boron carbide ceramics under high heating rate and high pressure," *Ceramic International 36(4),* pp. 1491-1494, 2010.

[52] Y. M. Maksimov, A. T. Pak, G. B. Lavrenchuk, Y. S. Naiborodenko and A. G. Merzhanov, "Spin Combustion of Gasless Systems," *Combustion, Explosion and Shock Waves,* vol. 15, pp. 415-418, 1979.

[53] Y. M. Maksimov, A. G. Merzhanov, A. T. Pak and M. N. Kuchkin, "Unstable Combustion Modes of Gasless Systems," *Combustion, Explosion and Shock Waves,* vol. 17, pp. 393-400, 1981.

[54] A. V. Dvoryankin, A. G. Strunina and A. G. Merzhanov, "Trends in the Spin Combustion of Thermites," *Combustion, Explosion and Shock Waves,* vol. 18, pp. 134-139, 1982.

[55] A. G. Strunina, A. V. Dvoryankin and A. G. Merzhanov, "Unstable Regimes of Thermite System Combustion," *Combustion, Explosion and Shock Waves,* vol. 19, pp. 158-163, 1983.

[56] B. V. Novozhilov, "The Theory of Surface Spin Combustion," *Pure and Applied Chemistry,* vol. 65, pp. 309-316, 1993.

[57] A. Bayliss, B. J. Matkowsky and A. P. Aldushin, "Dynamics of hot spots in solid fuel combustion," *Physica D 166,* pp. 104-130, 2002.

[58] T. P. Ivleva and A. G. Merzhanov, "Three-dimensional modes of unsteady solid-flame combustion," *Chaos: An Interdisciplinary Journal of Nonlinear Science 13(1),* pp. 80-86, 2003.

[59] E. A. Butakova and A. G. Strunina, "Thermophysical Properties of Some Thermite and Intermetallic Systems," *Combustion, Explosion and Shock Waves,* vol. 21, pp. 67-69, 1985.

[60] A. A. Zenin, A. G. Merzhanov and G. A. Nersisyan, "Thermal Wave Structure in SHS Processes," *Combustion, Explosion and Shock Waves,* vol. 17, pp. 63-71, 1981.

[61] C. A. Nunes, R. Sakidja, Z. Dong and J. H. Perepezko, "Liquidus Projection for the Mo-rich Portion of the Mo-Si-B Ternary System," *Intermetallics*, vol. 8, pp. 327-337, 2000.

[62] J. H. Perepezko, R. Sakidja, S. Kim and J. S. Park, "Multiphase Microstructures and Stability in High Temperature Mo-Si-B Alloys," in *Structural Intermetallics* 2001, Eds. K. J. Hemker, D. M. Dimiduk, H. Clemens, R. Darolia, H. Inui, J. M. Larsen, V. K. Sikka, M. Thomas and J. D. Whittenberger, (TMS, Warrendale, PA) 505 (2001).

Vita

Mohammad Shafiul Alam was born in Brahmanbaria, Bangladesh in 1988. He is the son of A. K. M. Abdur Rashid and Kohinoor Rashid. He grew up in Dhaka, Bangladesh and moved to El Paso after finishing undergraduate studies. Mohammad attended Khilgaon Government High School for ten years and graduated from Notre Dame College in 2005. In January 2006, Mohammad began his undergraduate studies at Bangladesh University of Engineering and Technology. In summer 2010, Mohammad worked in ACI Pharmaceuticals Ltd. as an intern and achieved hands-on experience in operation and performance of Generator, Compressor, Boiler, Chiller, Cooling Tower, and HVAC system. In February 2011, Mohammad received his B.Sc. degree in Mechanical Engineering. From June 2011 to June 2012, Mohammad worked in Star Particle Board Mills Ltd. as a Maintenance Engineer, Mechanical. In fall 2012, Mohammad started his M.S. studies at UTEP and became a member of Dr. Evgeny Shafirovich's research team in the Center for Space Exploration Technology Research, where he worked for the DOE-sponsored project on mechanically activated combustion synthesis of $MoSi_2$-based composites. Mohammad's research results were presented at the 8th US National Combustion Meeting in May 2013, the XII International Symposium on Self-propagating High-temperature Synthesis in October 2013, the 2014 Spring Technical Meeting of the Central States Section of the Combustion Institute in March 2014, and at the project review meetings conducted by the National Energy Technology Laboratory in 2013 and 2014. A full-length article, titled "Mechanically Activated Combustion Synthesis of Molybdenum Silicides and Borosilicides for Ultrahigh-Temperature Structural Applications," has been accepted for publication in a prestigious peer-reviewed journal *Proceedings of Combustion Institute* (published online in June 2014, will appear in Vol. 35). Mohammad will also present this paper at the 35th International Symposium on Combustion in San Francisco, CA (August 3-8, 2014).

Permanent address: 1419/3/A Khilgaon
Dhaka-01219
Bangladesh.

This thesis was typed by Mohammad S Alam.